Science Advances
AAAS

advances.sciencemag.org/cgi/content/full/6/6/eaav7416/DC1

Supplementary Materials for

Prior acquired resistance to paclitaxel relays diverse EGFR-targeted therapy persistence mechanisms

Mark Borris D. Aldonza, Jayoung Ku, Ji-Young Hong, Donghwa Kim, Seung Jung Yu, Min-Seok Lee, Monica Celine Prayogo, Stephanie Tan, Dayeon Kim, Jinju Han, Sang Kook Lee, Sung Gap Im, Han Suk Ryu, Yoosik Kim*

*Corresponding author. Email: ysyoosik@kaist.ac.kr

Published 7 February 2020, *Sci. Adv.* **6**, eaav7416 (2020)
DOI: 10.1126/sciadv.aav7416

This PDF file includes:

Supplementary Methods

Animal studies. All animal use and care followed the guidelines approved by the Institutional Animal Care and Use Committee of KAIST and Seoul National University. 4-week-old male athymic mice (BALB/c-nu) were purchased from Orient Bio Inc. and were transferred, established, and bred in an animal facility at GSMSE, KAIST and fed with free access to standard diet (PMI LabDiet) and water. A549 and A549-PTXR cell suspensions (1.2×10^7 cells) in 200 µL culture medium/growth factor-reduced Matrigel (BD Biosciences) in a 1:1 ratio were subcutaneously injected into the right flank of each mouse (except in KRAS RNAi cohort; see details below). Mice were treated when their tumor volumes reached 70 to 100 mm^3 (gefitinib cohort) and 100 to 150 mm^3 (paclitaxel cohort). Mice were randomized into vehicle control and treatment groups of four to five animals per cohort. Gefitinib (100 and 200 mg/kg body weight) and paclitaxel (10 mg/kg body weight) were dissolved in 200 µL vehicle solution (Tween 80-EtOH-H_2O in 1:1:98 ratio) and were orally administered to mice in appropriate cohorts once daily for 20 days (paclitaxel cohort) and 14 days (gefitinib cohort), respectively. The control group was treated with an equal volume of vehicle. Tumor volume was determined using digital caliper measurements, monitored for 37 days (paclitaxel cohort) and 22 days (gefitinib cohort), respectively, and calculated using the following formula: tumor volume = $(D \times d^2)/2$, in which D and *d* refer to the long and short tumor diameter, respectively. The body weight of each mouse was also monitored for toxicity. For the metastasis model, 7-8 week-old C57BL/6 male mice were purchased from Orient Bio Inc. LLC and LLC-PTXR cell suspensions (1.5×10^6 cells) in 140 µL culture medium were intravenously injected through the tail vein. Mice were sacrificed at days 15 and 37 after injection. Lung, liver, and spleen that developed primary or metastasized tumors were collected in ice-cold PBS for further testing. All animals were fed with free access to standard diet (PMI LabDiet) and water. All mice were maintained under continuous sedation by administering 2-4% isoflurane via an anesthesia mask during surgery and prior to euthanasia.

Resistance potential assay. Two confluent 150-mm plates per cell line were exposed to calculated IC_{10} value for each drug used for 36 h (paclitaxel, GSK269962A, docetaxel, epothilone B, vinblastine, PF-562271). Drug-stressed cells were plated $1x10^5$ cells per well of 6-well plates and were further treated with the IC_{10} drug concentrations for 72 h. Cells were cultured for another 24 h in drug-free media. Cells were subjected to escalating drug concentration selection (IC_{10} for 72 h, IC_{25} for 48 h, and IC_{50} for 24 h). Cells that underwent this selection were subjected to two protocols of expansion: for protocol 1, a drug-selected cell colony was picked and allowed to expand for 8 days in a drug-free media. For protocol 2, drug-selected colonies (from at least 3 well-spaced colonies) were picked and admixed in drug-free media prior to expansion for 7 days in a drug-free media. Prior to viability measurements, expanded cells (equal number per cell line) were seeded on a 96-well plate and allowed to adhere for 12 h. For gefitinib co-resistance potential assay, expanded cell lines from paclitaxel (both from protocols 1 and 2) were further subjected to drug-free expansion for 4 days and were tested for gefitinib sensitivity (2 µM gefitinib for 24 h). All viability measurements were assayed using SRB. Viability signatures were validated by MTT assay.

Immunohistochemistry. FFPE tissue sections were deparaffinized in xylene alternative (Histo-Clear, EMS; 3 × 5 min) and rehydrated in EtOH/H_2O gradient series (100%, 95%, 70%, 40%, 5 min each). The rehydrated slides were then washed in TBS (at least 10 min). Epitopes were unmasked using heat-induced retrieval method with the use of pre-heated Tris (10 mM Tris Base, 0.05% Tween 20, pH 8.0) and Citrate buffers (10 mM Sodium Citrate,

0.05% Tween 20, pH 6.0). Slides were pressure-cooked for 12 minutes in the Tris buffer, transferred to the Citrate buffer, heated for another 12 minutes, cooled to room temperature for 40 min, and then washed once with TBS containing 0.1% Tween-20 for 10 min. Tissue sections were permeabilized with 0.3% Triton X-100 in TBS for 45 minutes and then washed in TBS (2 × 5 min). Endogenous peroxidase activity was quenched in a peroxidase solution (0.3% H_2O_2 in TBS) and tissue sections were blocked in a universal blocking solution (10% normal donkey serum in 1% BSA/TBS) for at least 2 h. Slides were blotted to remove the serum and then primary antibodies were applied at predetermined concentrations (1:100 to 1:500) following manufacturer's recommendations. Slides were incubated overnight at 4 °C in a humidified chamber and then washed with TBS (3 × 5 min). Appropriate biotinylated link and horseradish peroxidase (HRP)-conjugated secondary antibodies were applied onto the tissue sections and were further incubated for up to 2 h in a dark humidified chamber at room temperature followed by washing. The slides were counterstained with hematoxylin as indicated, and dehydrated in EtOH/H_2O gradient series. The positive staining density was measured using a computerized imaging system composed of a Leica CCD camera connected to a Leica DMi1 microscope (Leica Microsystems). The H-score scoring system was used, which evaluated staining intensity (0 to 3) and the percentage of positively stained cells (0 to 1), with a final score ranging from 0 to 3. Representative images (Fig. 6C, right panel) were transformed by Fiji/ImageJ to correct for tritanope dichromacy due to variable bluish-yellowish background of acquired raw images. Replicate slides were also stained with H&E (Vector Labs) according to the manufacturer's protocol. A PVP- or toluene-based organic mountant was used to mount the slides.

Cell cycle analysis. The cells were harvested, washed twice, and fixed in 70% cold ethanol overnight at -20ºC. Ethanol-fixed cells were pelleted, washed with ice-cold PBS, and resuspended in staining solution containing 50 µg/mL PI, 0.1% Triton-X-100, 0.1% sodium citrate, and 100 µg/mL RNase. After 1 h of incubation at room temperature in the dark, the fluorescence-activated cells were sorted and cellular DNA content was analyzed by fluorescence-cell activation sorting using FACSCalibur flow cytometer (BD Biosciences) equipped with an argon laser and data were evaluated using CellQuest 3.0.1 software (Becton-Dickinson). At least 20,000 cells were used for each analysis. Changes in the percentage of cell distribution at each phase of the cell cycle were determined. The proportion of cells in different phases of the cell cycle was determined in triplicate and expressed as mean ± SD.

BrdU incorporation. A colometric BrdU incorporation assay (Abcam) was conducted to measure the rate of DNA synthesis. BrdU was added onto cells cultured in microplates followed by 4 h incubation to incorporate BrdU into the DNA of proliferating cells. Culture supernatant was removed followed by fixation. Cells were then incubated with an anti-BrdU antibody conjugated to peroxidase. Bound BrdU was detected by a substrate reaction and quantified by absorbance measurement at 350 nm.

3D invadopodia assay. Collagen mixtures were prepared by adding 10× PBS, ice-cold 1 N NaOH and media to rat tail type I collagen (BD Biosciences) to a final concentration of 2.5 mg/ml and pH 7.4. The mixtures were centrifuged (3 min, 10,000 × g, 4 °C) to eliminate air bubbles and placed on ice until use. A cover slip in a culture dish was first covered with 150 µl of collagen solution for the bottom layer, which was allowed to gel at 37 °C for 45 min. A cell suspension containing 1×10^5 cells/100 µl was mixed with 100 µl of collagen solution, loaded onto the bottom layer and allowed to gel at 37 °C for 45 min. Culture medium was then added to the dish, and the cells were incubated for 3 days prior to compound treatment. The embedded cells were observed under an inverted phase contrast light microscope or subjected directly for fixation and immunocytochemistry.

3D culture immunofluorescence. For the immunofluorescence of cells cultured in our in-

house built polymeric thin-film-based 3D culture and stacked collagen type I, cells with fixed with an ice-cold methanol/acetone (1:1) solution for 20 min at 4°C. Fixed cells were washed in a PBS wash solution containing 0.02% BSA and then permeabilised with 1% Triton-X100 (in PBS) for 5 min at RT. Permeabilised cells were washed multiple times with the wash solution. Cells were then blocked in blocking solution containing 5% normal goat serum (NGS), 1% BSA and 0.2% Triton- X100 for 15 min at RT. Cells were then subjected for antibody detection and counterstaining with indicated dyes. Cells were usually primed for antibodies for 2 h at RT.

Senescence assays. Senescence is a complex phenotype. To date, there are no true senescence-specific markers yet established. Therefore, we depended on a panoply of markers and phenotypes known to be displayed by senescent cells. SA-β-gal activity was detected using Senescence β-Galactosidase Staining Kit (CST) following manufacturer's protocol. SA-β-gal positive cells were quantified based on three independent images from different regions of the staining as analyzed by digital inverted light microscopy (40x phase-contrast; Leica DMi1). For fluorescent SA-β -gal labelling, cells were incubated with 100 nM bafilomycin A1 and 100 µM DDAO galactoside (9H-(1,3-Dichloro-9,9-Dimethylacridin-2-One-7-yl) β-D-Galactopyranoside) for 2 h at standard culture conditions. Cells were washed with PBS, fixed in 0.5% glutaraldehyde solution in PBS (pH 5.5; with 1 mM MgCl2) for 15 min and nuclei were stained with DAPI before image acquisition. Cells were imaged by confocal microscopy. For colony formation, colony-forming units from 10^2-seeded cells were grown in 3 mL of H4100 methylcellulose medium (Stem Cell Technologies) for indicated long-term culture (cells were replenished with fresh medium every 4 days). Colonies were stained with 0.01% crystal violet. Clusters of greater than 50 cells were scored as colonies, using bright-field or fluorescence microscopy. For measuring SASP activity, we evaluated the gene expression of its components IL-1α, IL-6, Mmp-3, Mmp-9, Cxcl-1, Cxcl-10 and Ccl20 by qPCR.

Cell invasion assay. Chemotactic invasion assay was carried out in Boyden chamber wells (24-well format, 8 µm pore size, Corning) with matrigel/ECM-based membrane. Matrigel matrix (Corning) was diluted to 1 mg/mL with serum-free culture medium and applied on the insert in the upper chambers. For chemotaxis induction of cells, 800 µL of culture medium supplemented with 10% FBS was added to the lower chambers. After incubation for 24 h at standard culture conditions, the membrane inserts were removed and the non-invading cells were removed from the upper surface of the membrane. Invaded cells were stained with 0.1% crystal violet for 20 min and washed with water. The cells were imaged by digital inverted light microscopy. The invading cells were counted in five random fields.

Caspase activity assays. Caspases 3/7 and 9 activities were assessed using a fluorescence-based Apo-ONE Homogeneous Caspase-3/7 Assay Kit (Promega) and luminescence-based Caspase-Glo 9 Assay System (Promega), respectively, following manufacturer's protocol. Briefly, 2.5 x 10^4 cells were seeded onto 96-well plates, allowed to adhere overnight, and treated according to indicated drug schedules. 120 µL of master reagent (mix of kit's substrate and buffer) was loaded onto each well, gently mixed in a shaker for 1 min, and incubated for 40 min to 90 min at RT. Excitation and emission wavelengths were set at 560 and 590 nm, respectively. Luminescence was read on POLARstar Omega luminometer.

***Ex vivo* biochemical analysis of tumors.** Following surgery, xenograft tumors were flash-frozen in liquid nitrogen. A portion of the frozen tumor excised from each of the nude mice was thawed on ice and homogenized in Complete Lysis Buffer (Active Motif) for whole lysate extraction or in RLT-ME buffer (Qiagen) for total RNA isolation using a handheld

homogenizer. The protein concentrations of the tumor lysates were determined using Bio-Rad Protein Determination Kit (Bio-Rad) and aliquots were stored at −80°C. RNA was extracted using RNeasy Mini Kits (Qiagen) following manufacturer's protocol. Lysates were subjected to Western blotting and total RNA was subjected to RT-PCR and qPCRs. Excised portions of primary/metastasized tumor nodules in organs from mice were thawed on ice and homogenized in Complete Lysis Buffer using a handheld homogenizer. Tumor lysates were subjected to immunoblotting and phosphorylation assay as described. Whole RNA from tumor samples was isolated from cells using RNAeasy Mini Kit according to manufacturer's instructions and was subjected to RT-PCR as described.

ELISA-based kinase and phosphorylation assays. Tyrosine 1068 phosphorylation of EGFR and kinase activities of total EGFR, AKT1, and ERK1/2 were assessed by solid phase sandwich ELISA (CST PathScan® kits) following manufacturer's protocol. The assay quantitatively detects endogenous levels of the indicated targets.

Drug efflux assays. For P-gp ATPase activity assay, we used the luminescent Pgp-Glo Assay System (Promega) following the manufacturer's protocol. Samples treated with Na3VO4 (negative substrate; inhibition) and verapamil (positive substrate; stimulation) served as controls. MgATP standards were used to facilitate the conversion of sample relative light units (RLU) to ATP concentrations (although not necessary to measure fold changes in activity). Luminescence was read on POLARstar Omega luminometer (BMG LABTECH). For intracellular rho-123 uptake assay, cells were incubated with 5.5 μM of rho-123 for 30 to 45 min in the presence or absence of verapamil at standard culture conditions. Cells were then lysed and intracellular accumulation of rho-123 was determined by spectrofluorometry (VERSAmax microplate reader; Molecular Devices). Excitation and emission wavelengths were set at 485 and 535 nm, respectively.

MET copy number and genomic amplification analysis. Genomic DNA was purified using the DNA easy kit (Qiagen) following manufacturer's instructions with minor modifications (lysis and high salt/ethanol precipitation steps were scaled up). Genomic DNA was stored in TE (10 mM Tris-HCl, 1 mM EDTA). In evaluating MET copy number, a qPCR-based detection was performed by comparing the MET locus to the reference LINE-1, a repetitive element for which copy numbers per haploid genome are similar among all of the human normal and neoplastic cells and the most abundant autonomous retrotransposon in the human consisting of 17% of the genome, in the genomic DNA of the samples. MET primer sequence was designed to generate a 145-bp amplicon in exon 2. Using this designed sequence, relative copy number was determined by comparing ratio of MET locus to LINE-1 per cell line with the ratio of these genes in normal human genomic DNA (Novagen, Merck) as a diploid control to validate uniqueness. Primer sets for both MET and LINE-1 were confirmed to generate a single anticipated size amplicon visualized on a 3% agarose gel stained with an ethidium bromide alternative. Primer sequences for MET and LINE-1 are: forward; 5′-ATC AAC ATG GCT CTA GTT GTC-3′, reverse; 5′-GGG AGA ATA TGC AGT GAA CC-3′, and forward; 5′-AAA GCC GCT CAA CTA CAT GG-3′, reverse; 5′-TGC TTT GAA TGC GTC CCA GAG-3′, respectively. To validate our calculated ratios, we also chose Ribonuclease P (forward; 5′-AGA TTT GGA CCT GCG AGC G-3′, reverse; 5′-GAG CGG CTG TCT CCA CAA GT-3′) as another single-copy reference gene, encoding the RNA moiety for the RNase P enzyme. For genomic amplification analysis, a fluorogenic MGB probe for MET was used (VIC-TGG ATA ATT GTG TCT TTC TCT AG-MGBNFQ). PCR reactions were carried out as described previously. Each amplification reaction was checked for the absence of nonspecific PCR products by dissociation-curve analysis. PCRs for each primer set were performed in triplicate, and mean values were calculated. Quantification was based on the standard curve method.

ATP measurement. Cells were seeded in 96-well plates and were subjected to indicated

treatment/culture conditions all in nutrient-restricted media (10% FBS dialyzed against 0.15M NaCl until <5 mg/dL glucose, 10,000 MW dialysis tubing, and no L-glutamine). ATP levels were measured using the luminescence-based ATPLite system (Perkin-Elmer) following manufacturer's instructions.

KRAS RNAi, copy number analysis, and restriction fragment length polymorphism (RFLP) analysis. For RNAi, siRNAs targeting total KRAS and mutant KRAS were designed and purchased from Genolution Pharmaceuticals. All cells were reverse-transfected with RNAiMax reagent (Invitrogen) or FuGene 6 transfection reagents (Promega) according to the manufacturer's instructions, using siRNA molecules at a final concentration of 10-20 nM. Media was changed 6 hours following transfections to minimize toxicity. The siRNA sequences used for KRAS siRNA experiments are: 5′-UUC UCC GAA CGU GUC ACG U-3′ (sense) and 5′-ACG UGA CAC GUU CGG AGA A-3′ (anti-sense) for siControl, 5′-CAG CUA AUU CAG AAU CAU U-3′ (sense) and 5′-AAU GAU UCU GAA UUA GCU G-3′ (anti-sense) for siKRAS. Experiments were performed 60 to 72 h post transfection as Western blotting indicated protein depletion to background levels. For copy number analysis, a qPCR-based detection was adapted by evaluating *KRAS* copy number in each sample, comparing the *KRAS* locus to the reference *LINE-1*, a repetitive element for which copy numbers per haploid genome are similar among all of the human normal and neoplastic cells. Genomic DNA was prepared as mentioned above. Since we were not able to avail commercially available (if there is any) mutant-specific KRAS antibodies, we used a PCR-based RFLP analysis to verify that our KRAS RNAi can target homozygous and heterozygous codon 12 mutant KRAS. Following total RNA extraction, cDNA was synthesized using 4 μg of total RNA with the SuperScript II First-Strand Synthesis using oligo (dT) primer System (Invitrogen). Aliquots of this reaction were used for subsequent PCR amplification. The sense primer was designed to introduce a base substitution that created a BstNI recognition site for the wild-type codon 12 (GGT) but not for the codon 12 with the KRAS mutation. The PCR products were digested with the restriction enzyme BstNI (30~40 units, New England Biolabs) at 60°C for 3 h in a final volume of 60 μL. Products were electrophoresed and visualized on 3% agarose gel stained with an ethidium bromide alternative. Upon incubation with BstNI, the fragments containing WT allele produced a 156-bp DNA fragment (H1299 cell) whereas the mutant allele remains uncut to produce a 186-bp DNA fragment (A549- and H358-derived cells). Note that fragments containing homozygous G12S produced a single band whereas those containing heterozygous G12C mutations produced double bands.

Generation and expansion of gefitinib persisters derived from *EGFR*-mutant cell lines. $4x10^5$ PC9 or HCC827 cells were plated in 150 mm plates and allowed to adhere for 18 h. Cells were then treated with 0.4 μM (for PC9) or 0.04 μM gefitinib (for HCC827) initially for 6 days followed by 1 μM (for PC9) or 0.1 μM gefitinib (for HCC827) treatment for 12 days. Fresh media containing drug was replaced every 3 days until clones of drug-resistant cells appeared. At day 20 of drug selection, ~42 clones per plate (average from 150 mm plates) appeared. Isolated clones were individually expanded in drug-containing media, and when necessary, stocked in 1:1 FBS+10%DMSO:drug-containing media. These initially expanded clones were maintained in minimally tolerated concentrations of gefitinib, replenished every 3 days.

Bioinformatics. For co-occurrence gene analysis, we used the data from the Pan-Lung Cancer TCGA cohort. We stratified the co-occurring genes in patients with FOXO3a-amplified or -deep-deleted expressions. We identified how many in these co-occurring genes are related with the EMT and CSC phenotypes. We used the functionally annotated genes in the dbEMT (http://dbemt.bioinfo-minzhao.org/) and CSCdb (http://bioinformatics.ustc.edu.cn/cscdb/) databases, which are comprehensive gene resources for EMT and CSC, respectively.

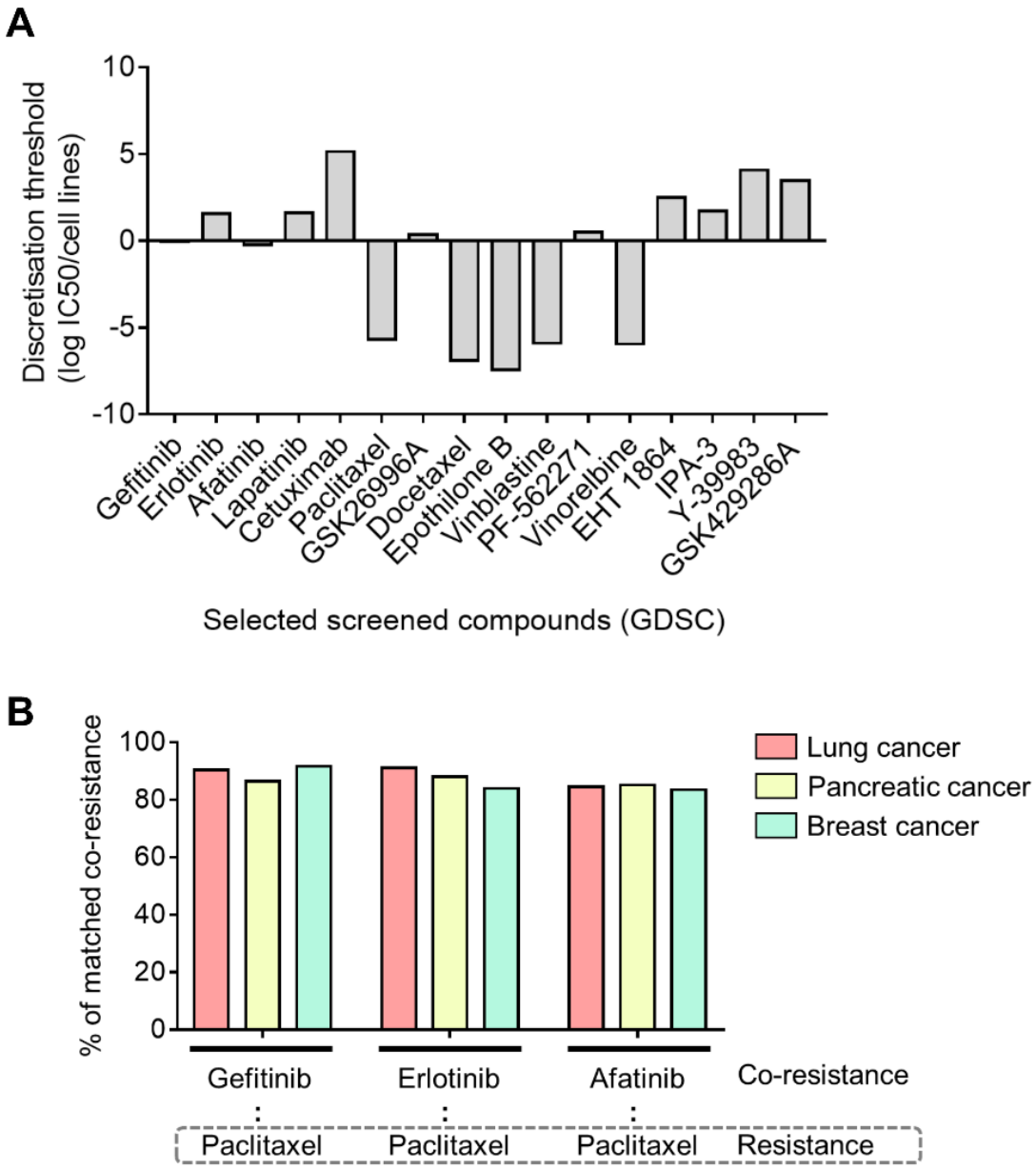

Fig. S1. GDSC parameters on selected compounds. (**A**) Discretization threshold profile of indicated EGFR-TKIs and antimitotic drugs. These threshold values corresponded to three standard deviations above/below the mean of the normalized scores based on the LOBICO drug response prediction analysis in the GDSC. The output feature was the response of the cancer cell lines to an anticancer drug as measured by the IC_{50}. (**B**) Cancer type categorization of GDSC cell lines classified to be resistant to paclitaxel and co-resistant to indicated EGFR-TKIs.

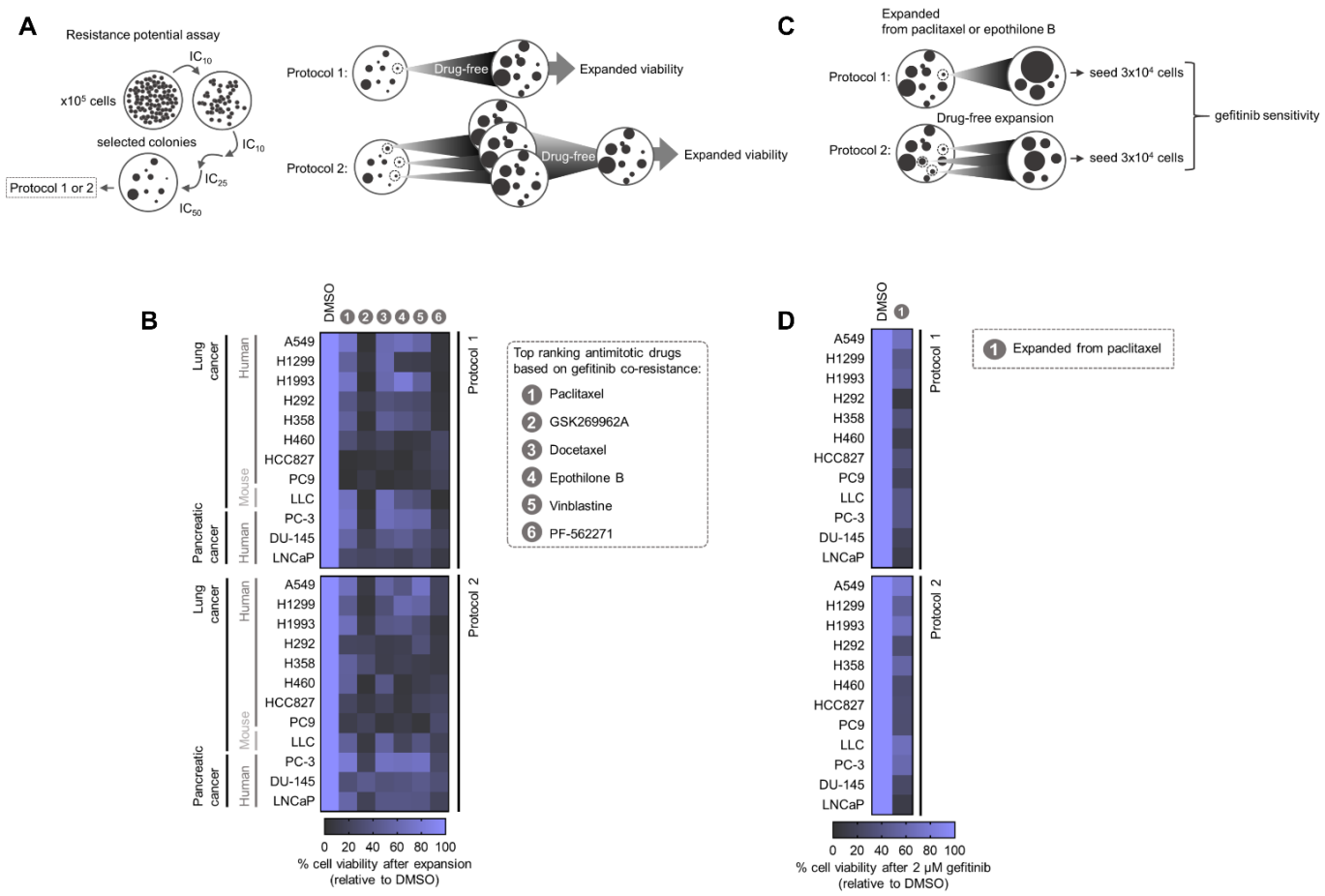

Fig. S2. Resistance potential assay on all parental cell lines used in the study. (**A**) Experimental strategies (two protocols; expansion from single colony or multiple colonies) to screen for cell lines with potential to develop resistance to indicated antimitotic drugs with high gefitinib co-resistance signature as classified in the GDSC. See also Supplementary Methods. (**B**) Characterization of viability of indicated cell lines upon specific drug-specific selection and expansion protocols schemed in A (top six antimitotic drugs with highest co-resistance signature with gefitinib). Cells were assayed for SRB. Representative of two independent experiments. (**C**) Schematic of gefitinib resistance potential assay. (**D**) Characterization of viability of cells as in B except only expanded from paclitaxel (antimitotic drug with highest resistance potential across our 12 parental cell line panel) upon gefitinib selection and expansion protocols schemed in C. Cells were assayed for SRB. Representative of two independent experiments.

A

Species	Tissue disease type	Parental sensitive line	Paclitaxel resistance	Establishment (approx. weeks)	Expanded from colonies?	Initial → final conc. (nM)	Weekly drug maintenance (nM)
Human	Lung adenocarcinoma	A549	Stable (PTXR)	52	No	40 → 16,000	100
Human	Lung adenocarcinoma	A549	Transient (PTXP)	5	Yes	40 → 4,000	20
Human	Prostate adenocarcinoma	DU-145	Stable (PTXR)	24	No	4 → 400	70
	Lung adenocarcinoma	HCC827	Transient (PTXP)	3	Yes	0.0001 → 10	2
Human	Lung carcinoma	H1299	Stable (PTXR)	35	No	20 → 2,000	70
Human	Lung adenocarcinoma	H1993	Stable (PTXR)	34	No	4 → 1,000	80
Human	Lung carcinoma	H292	Stable (PTXR)	26	Yes	10 → 2,000	100
Human	Lung adenocarcinoma	H358	Stable (PTXR)	30	No	2 → 600	60
Human	Lung adenocarcinoma	H460	Stable (PTXR)	21	No	5 → 200	50
Mouse (C57BL)	Lewis lung carcinoma	LLC1 (LL/2)	Transient (PTXP)	7	Yes	5 → 1,500	80
Mouse (C57BL)	Lewis lung carcinoma	LLC1 (LL/2)	Stable (PTXR)	40	No	20 → 10,000	150
Human	Prostate carcinoma	LNCaP clone FGC	Stable (PTXR)	21	Yes	100 → 18,000	120
Human	Prostate adenocarcinoma	PC-3	Stable (PTXR)	42	No	8 → 8,000	100
Human	Prostate adenocarcinoma	PC-3	Transient (PTXP)	6	Yes	8 → 4,000	30
Human	Lung adenocarcinoma	PC9	Transient (PTXP)	4	Yes	0.001 → 20	5

C

Co-resistance of other microtubule-targeting drugs with paclitaxel (GDSC dataset)

Drug	Relative percentage	Co-resistance Rank (out of 265 drugs)
Epothilone B	98.63%	1
Vinorelbine	94.86%	16
Vinblastine	89.50%	94

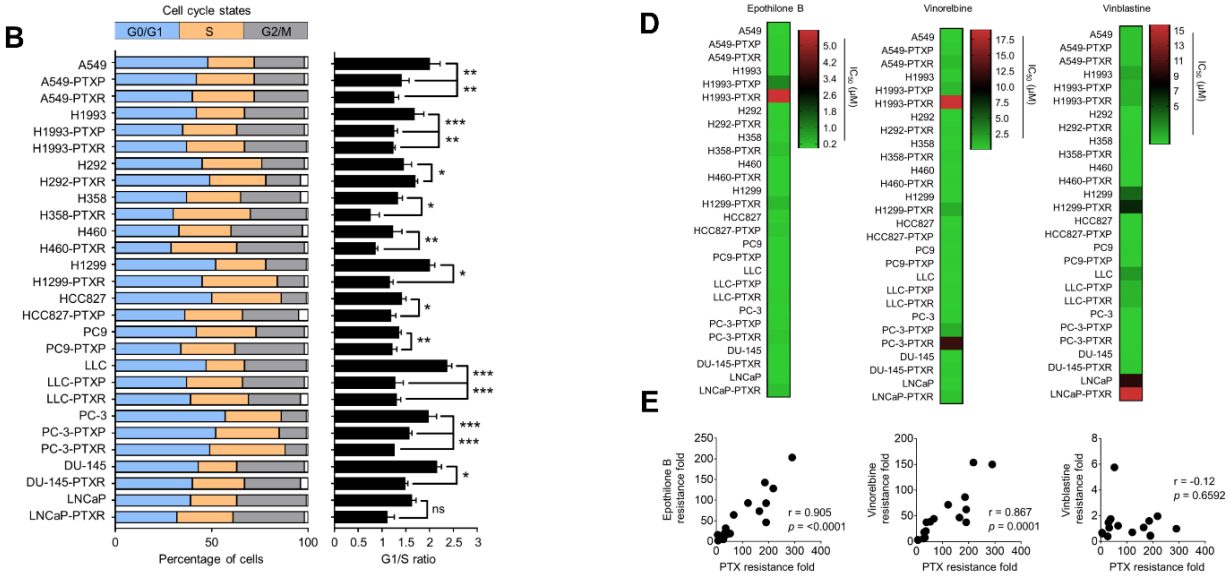

Fig. S3. Characterization of paclitaxel-resistant cancer cells for cell cycle progression and collateral resistance to other microtubule-targeting drugs. (**A**) Information on paclitaxel resistance selection in a panel of human and mouse cancer cell lines. (**B**) Cell-cycle states of 12 lines of parental cells, ten lines of PTXR cells, and six lines of PTXP cells (left) and their respective G1/S ratio (right). Representative of two independent experiments. **P*<0.05, ***P*<0.01, ****P*<0.005, Student's *t* test. (**C**) Data from the GDSC data set calculating the co-resistance signatures of epothilone B, vonorelbine, and vinblastine, with paclitaxel. (**D** and **E**) Validation of co-resistance of other microtubule-targeting drugs with paclitaxel. Cells were treated with or without drugs for 72 h with a concentration dilution series and were assayed for SRB. IC_{50}s (in μM) were then calculated. Representative of two independent experiments. Resistance fold for each drug was calculated per cell line and plotted for correlation.

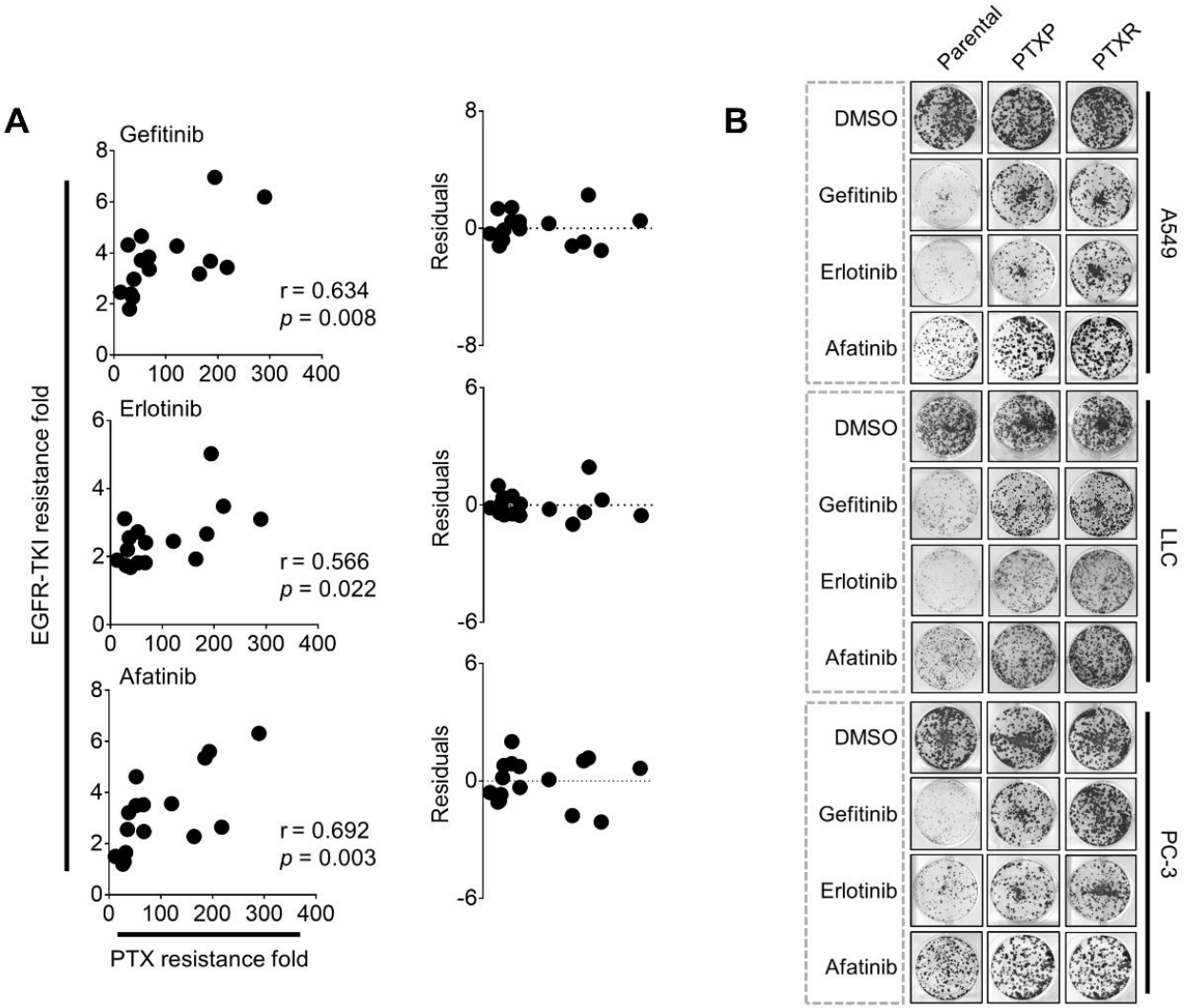

Fig. S4. Collateral EGFR-TKI resistance in paclitaxel-resistant cancer cells. (**A**) Correlation and residual analysis between collateral resistance to indicated EGFR-TKIs and resistance to paclitaxel in the same panel of cell lines as in Fig. 1F. (**B**) Colony formation assay of A549-, LLC-, and PC-3-derived parental and PTXR cells upon treatment with indicated EGFR-TKIs. Cells were treated with or without 2~5 μM of indicated drugs for 8 days followed by drug-free culture for 8 days. Representative of two independent experiments.

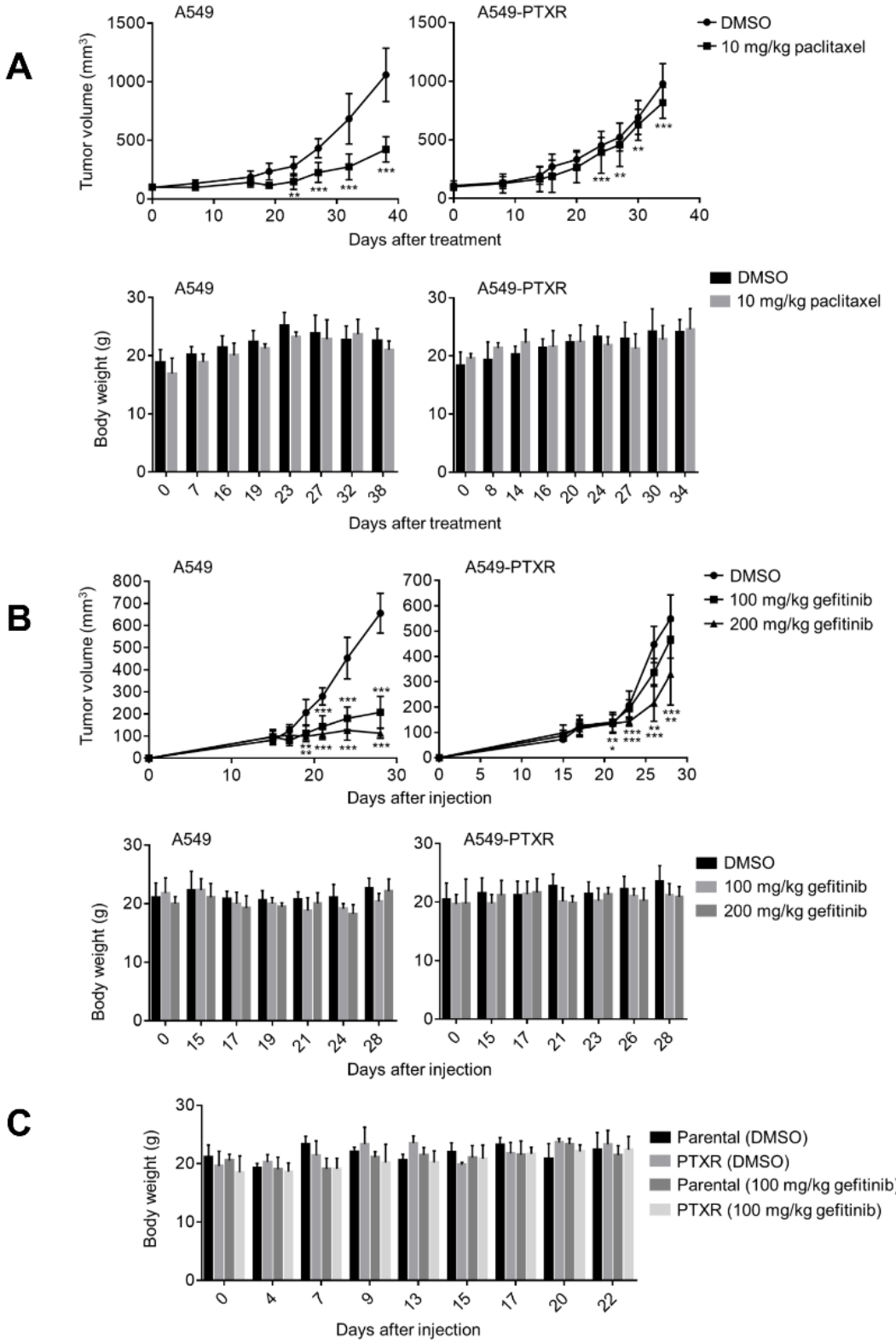

Fig. S5. Collateral gefitinib resistance in paclitaxel-resistant xenograft tumors. (**A**) Tumor growth of A549-derived parental and PTXR cells upon subcutaneous injection into flanks of nude mice. 10 mg/kg paclitaxel was administered orally once daily for 20 days (top panel). The control group was treated with an equal volume of vehicle. Tumor volume and body weight (bottom panel) were measured using digital calipers and weighing scale, respectively, every 2~3 days and indicated time points were selected for plotting (n=4 per group, two cohorts per cell line, mean±SD, **P*<0.05, ***P*<0.01, ****P*<0.001, Student's *t* test). (**B**) Tumor growth of the same panel of cells as in A except mice were treated with 100 mg/kg or 200 mg/kg of gefitinib. Gefitinib was orally administered once daily for 14 days. The control group was treated with an equal volume of vehicle. Tumor volume and body weight were measured and monitored as in A (n=4 per group, three cohorts per cell line, mean±SD, **P*<0.05, ***P*<0.01, ****P*<0.001, Student's *t* test). (**C**) Body weight measurements of mice used for KRAS RNAi cohorts. See fig. S19F.

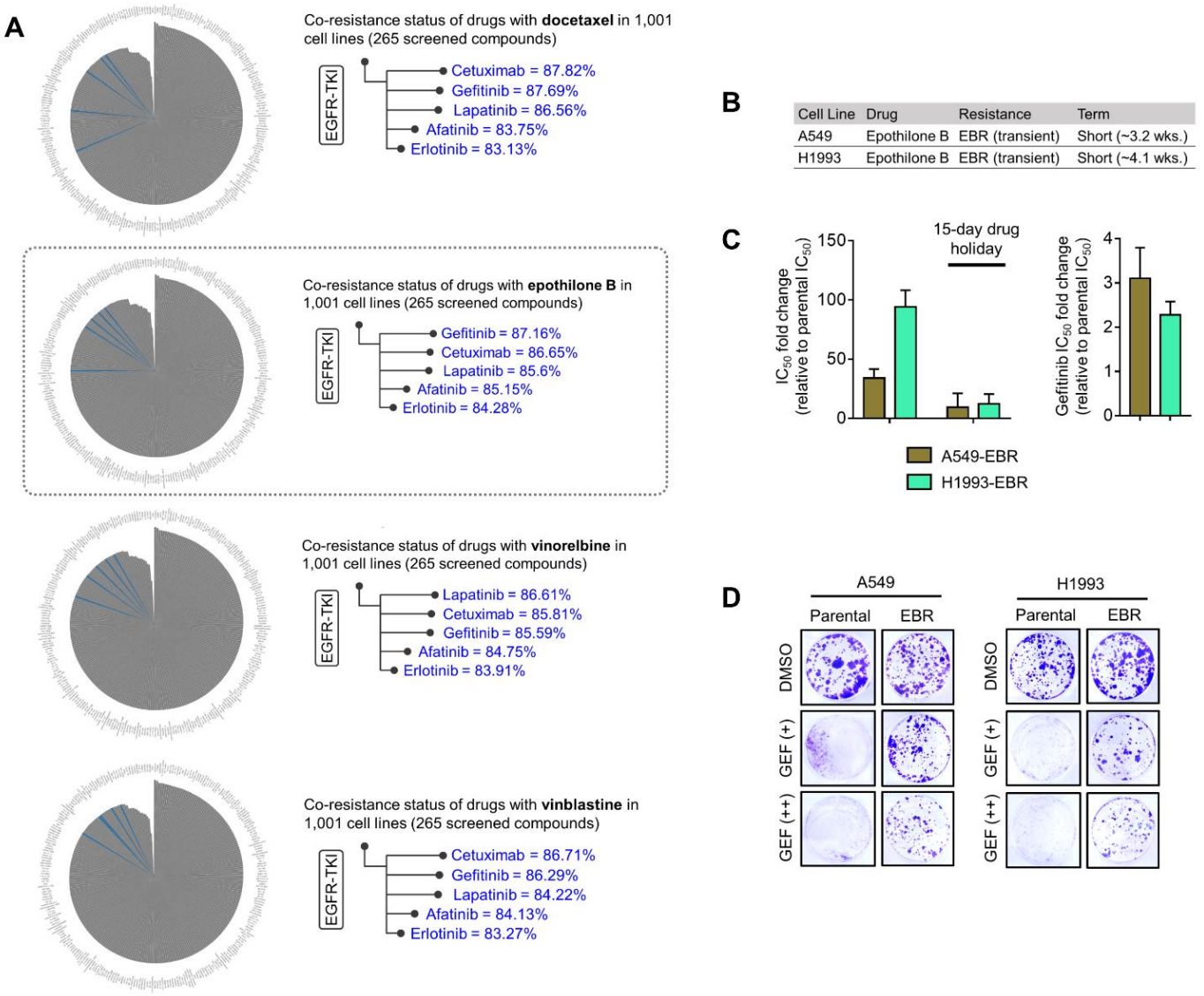

Fig. S6. GDSC-based coresistance ranking of some microtubule-targeting drugs with EGFR-TKIs and validation study using epothilone B–resistant cell lines. (**A**) Co-resistance ranking of five EGFR-TKIs (gefitinib, erlotinib, afatinib, lapatinib, cetuximab) in cancer cell lines resistant to indicated microtubule-targeting drugs (docetaxel, epothilone B, vinorelbine, vinblastine). Drugs were ranked as in Fig. 1B. (**B**) Transient epothilone B resistance lines (EBR) derived from A549 and H1993 cells. (**C**) Characterization of established epothilone B resistance and collateral gefitinib resistance in cell lines as in B. Stability and transience of resistance were assayed by employing a 15-day drug holiday. Cells were treated with or without drugs for 72 h with a concentration dilution series and were assayed for SRB. Resistance was assessed based on drug IC_{50} values. Representative of three independent experiments. (**D**) Colony formation of indicated A549- and H1993-derived cells. Cells were treated with or without 4 μM or 8 μM of gefitinib for 5 days followed by drug-free culture for 8 days. Representative of two independent experiments.

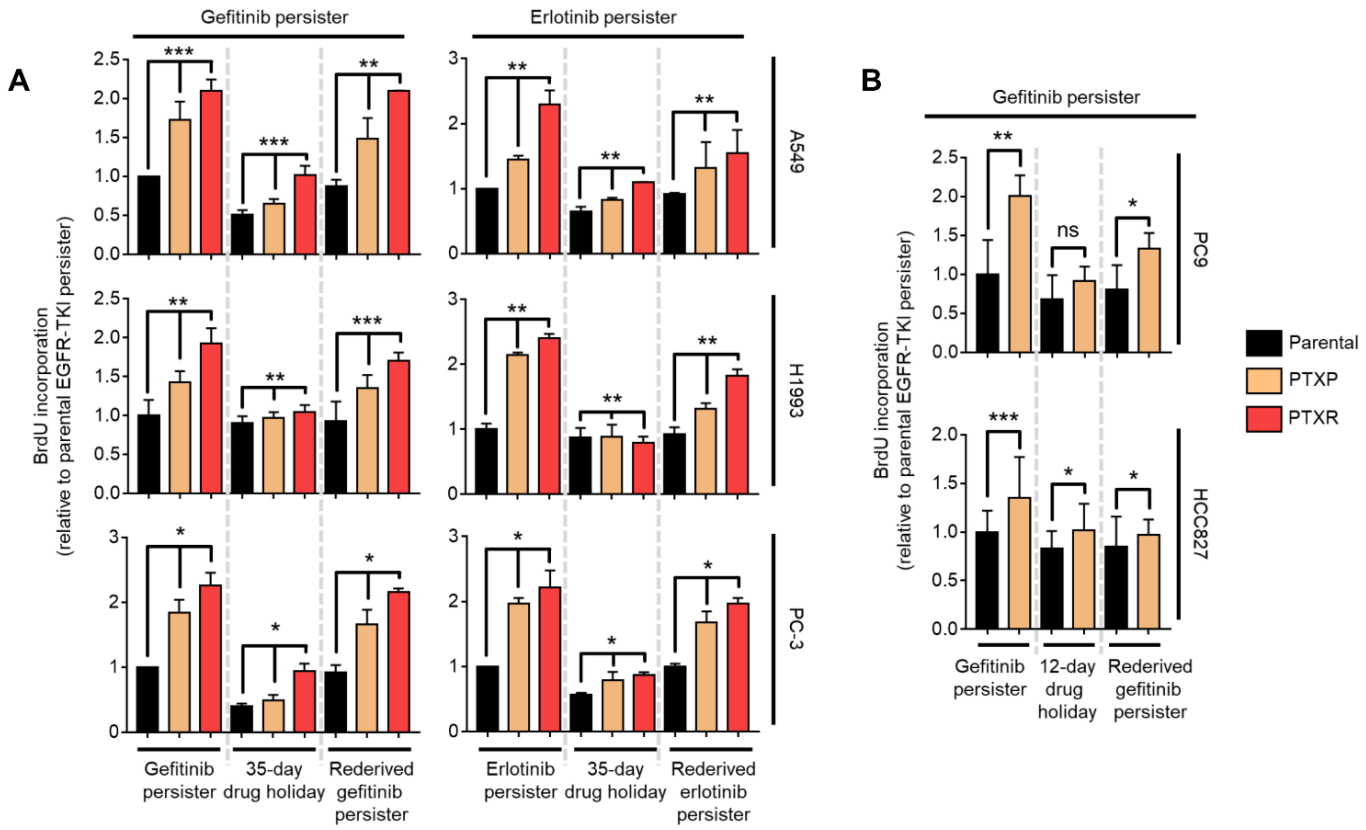

Fig. S7. BrdU incorporation assay on all EGFR-TKI persister models used in the study. (**A**) BrdU incorporation assay in indicated A549- and PC-3-derived EGFR-TKI persisters upon treatment with 8 μM gefitinib (for gefitinib persisters) or 10 μM erlotinib (for erlotinib persisters) for 5 days (mean±SD of three biological replicates, *P* values by Student's *t* test). (**B**) BrdU incorporation assay in indicated PC9- and HCC827-derived gefitinib persisters upon treatment with 1 μM gefitinib for 4 days (mean±SD of three biological replicates, *P* values by Student's *t* test).

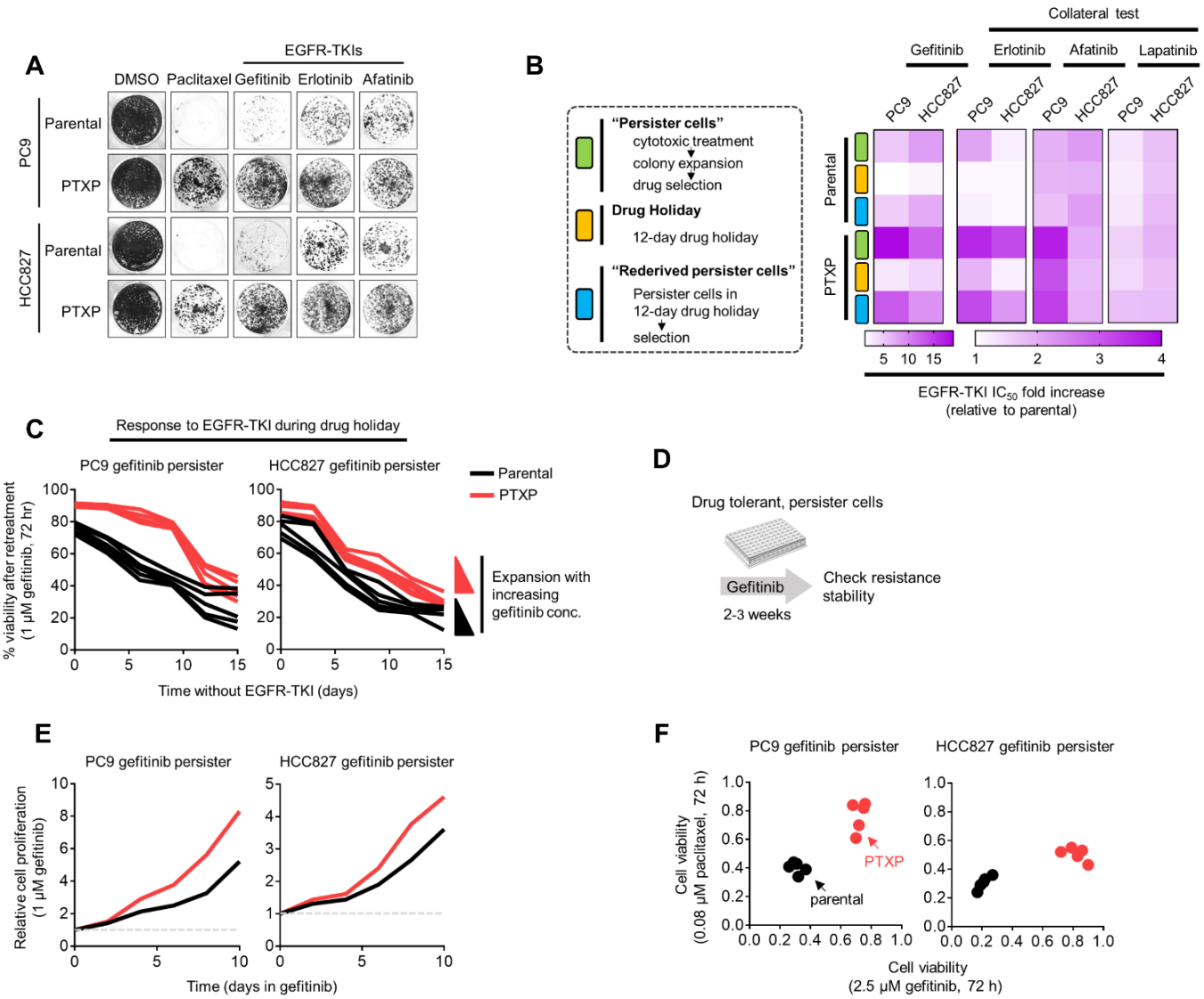

Fig. S8. Characterization of GPs derived from EGFR-TKI hypersensitive cell lines. (**A**) Colony formation assay of PC9- and HCC827-derived parental and PTXP cells upon treatment with or without 0.01~0.2 μM of indicated EGFR-TKIs for 6 days followed by drug-free culture for 12 days. Representative of two independent experiments. (**B**) Generation and characterization of reversible drug-tolerant, slow-growing PC9- and HCC827-derived gefitinib persisters in response to indicated gefitinib-induced selection, expansion, and drug holiday schedules in culture; assayed by SRB. IC_{50} values are relative to parental non-persisters. Representative of three independent experiments. (**C**) Evolution of established PC9- and HCC827-derived persisters to gefitinib during long-term drug holiday. Cells were grown in drug-free media and periodically retested over ~15 days for sensitization to EGFR-TKIs (retesting regime: 1 μM gefitinib, 72 h, assayed by SRB). Representative of two independent experiments. (**D** and **E**) Long-term growth of indicated gefitinib persisters after over ~2.5 weeks of step-wise selection to gefitinib to stabilize resistance. Cells were then retested upon treatment in 1 μM gefitinib at indicated times and were assayed by SRB. Values are relative to non-treated. Representative of two independent experiments. (**F**) Resistance status to both paclitaxel and gefitinib of PC9- and HCC827-derived persister pools generated as in D and expanded under increasing concentrations of gefitinib. Cells were treated with or indicated concentration of drugs for 72 h and were assayed by SRB.

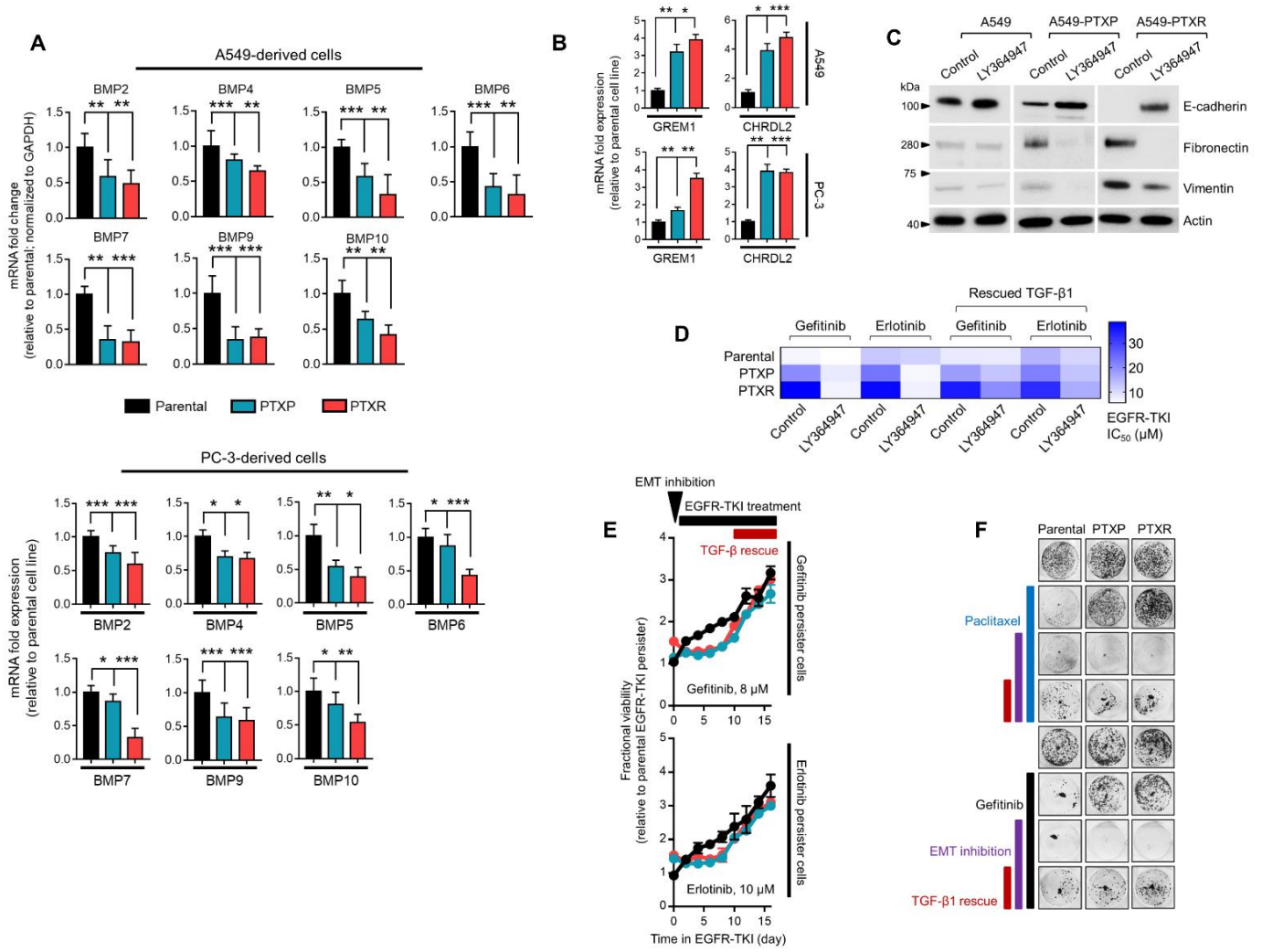

Fig. S9. Characterization of EMT profile. (**A**) qRT-PCR analysis of indicated BMP genes, which are antagonists of extracellular TGF-β signaling, in A549-derived and PC-3-derived cells. Values are relative to parental and were normalized to GAPDH levels (mean±SD of three biological replicates, **P*<0.05, ***P*<0.01, ****P*<0.005, Student's *t* test). (**B**) qRT-PCR analysis of indicated BMP antagonists in A549- and PC-3-derived cells. Values are relative to parental and were normalized to GAPDH levels (mean±SD of three biological replicates, **P*<0.05, ***P*<0.01, ****P*<0.005, Student's *t* test). (**C**) Western blot analysis of indicated EMT markers in A549-parental, -PTXP, and -PTXR cells upon treatment with or without 10 μM of TGF-β1-receptor antagonist LY364947 for 2 h (upper panel). Actin was used as a loading control. Representative of two independent experiments. (**D**) Sensitivity characterization of A549-parental, -PTXP, and -PTXR cells upon treatment with or without 10 μM LY364947 for 2 h followed by indicated EGFR-TKI treatment for 72 h with a concentration dilution series (lower panel). Rescue represents treatment with 5 ng/mL of recombinant human TGF-β1 for 48 h followed by same EGFR-TKI treatment (assayed by SRB). Representative of two independent experiments. (**E**) Sensitivity characterization of indicated A549-derived gefitinib and erlotinib persisters upon treatment with 10 μM of LY364947 for 8 h followed by long-term EGFR-TKI treatment and rescue with 5 ng/mL of recombinant human TGF-β1 as indicated. Values are relative to parental EGFR-TKI persisters (mean±SD of two biological replicates). (**F**) Colony formation assay of indicated A549-derived cells upon treatment with or without 10 μM of LY364947 for 2 h and rescue with 5 ng/mL of recombinant human TGF-β1 for 48 h followed by 4 nM paclitaxel or 2 μM gefitinib for 8 days then cultured for 4 days in drug-free media. Representative of two independent experiments.

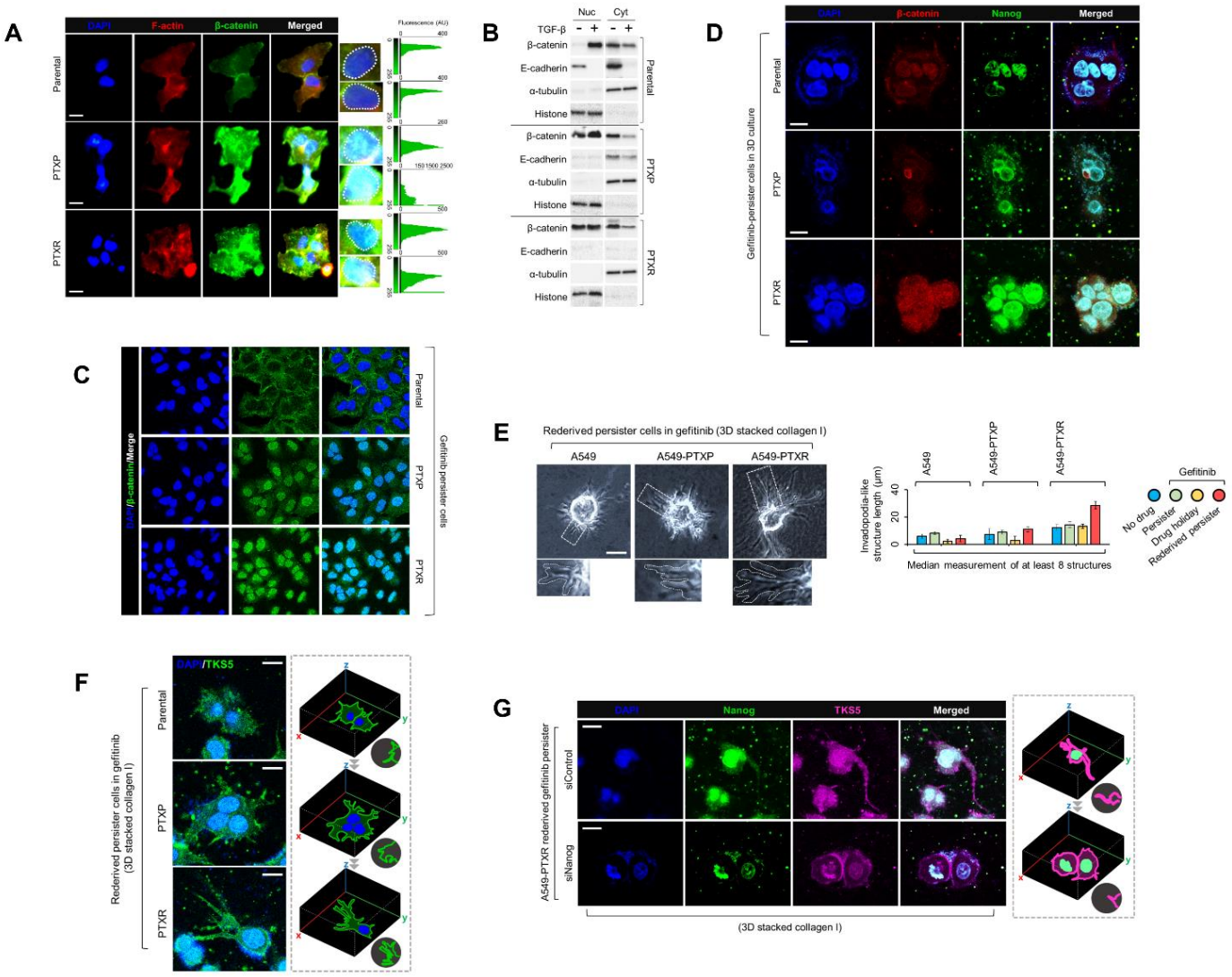

Fig. S10. β-Catenin translocation and invadopodia protrusion are correlated with stemness in GPs derived from paclitaxel-resistant cancer cells. (**A**) Representative images of β-catenin immunofluorescence (green) in indicated A549-derived cells. Cells were counterstained for F-actin (red) and DAPI (blue). Scale bar, 25 μm. Intensity of nuclear β-catenin was quantified using Fiji/ImageJ. (**B**) Western blot analysis of nuclear and cytoplasmic β-catenin and indicated markers in A549-derived cells upon treatment with or without recombinant human 5 ng/mL TGF-βI for 12 h. (**C**) Representative images of β-catenin immunofluorescence (green) in indicated A549-derived gefitinib persisters. Cells were counterstained for DAPI (blue). (**D**) Representative images of immunofluorescence of Nanog (green) and β-catenin (red) in indicated 3D culture-grown A549-derived gefitinib persisters after 2 days in culture. Cells were not re-plated to image the formation of 3D structures prior to sphere formation. Cells were counterstained for DAPI (blue). Scale bar, 100 μm. (**E**) Representative bright-field images (Axio Scope.A1) of A549 rederived gefitinib persisters cultured in 3D stacked collagen upon treatment with or without 5 μM gefitinib for 48 h and were cultured in drug-free media for 4 days. Scale bar, 90 μm. The length of these Invadopodia structures were measured using Fiji/ImageJ (median of >8 measurements). (**F**) Representative immunofluorescence of an invadopodia marker TKS5 (green) in indicated A549-derived rederived gefitinib persisters cultured as in F, except cultured for 4 days. Scale bar, 125 μm. Cells were counterstained for DAPI (blue). (**G**) Representative immunofluorescence of TKS5 (magenta) and Nanog (green) in indicated A549 rederived gefitinib persisters cultured as in F upon Nanog RNAi for 48 h. Cells were transfected prior to 3D collagen stack culture. Scale bar, 125 μm. Cells were counterstained for DAPI (blue). Representative of three independent experiments.

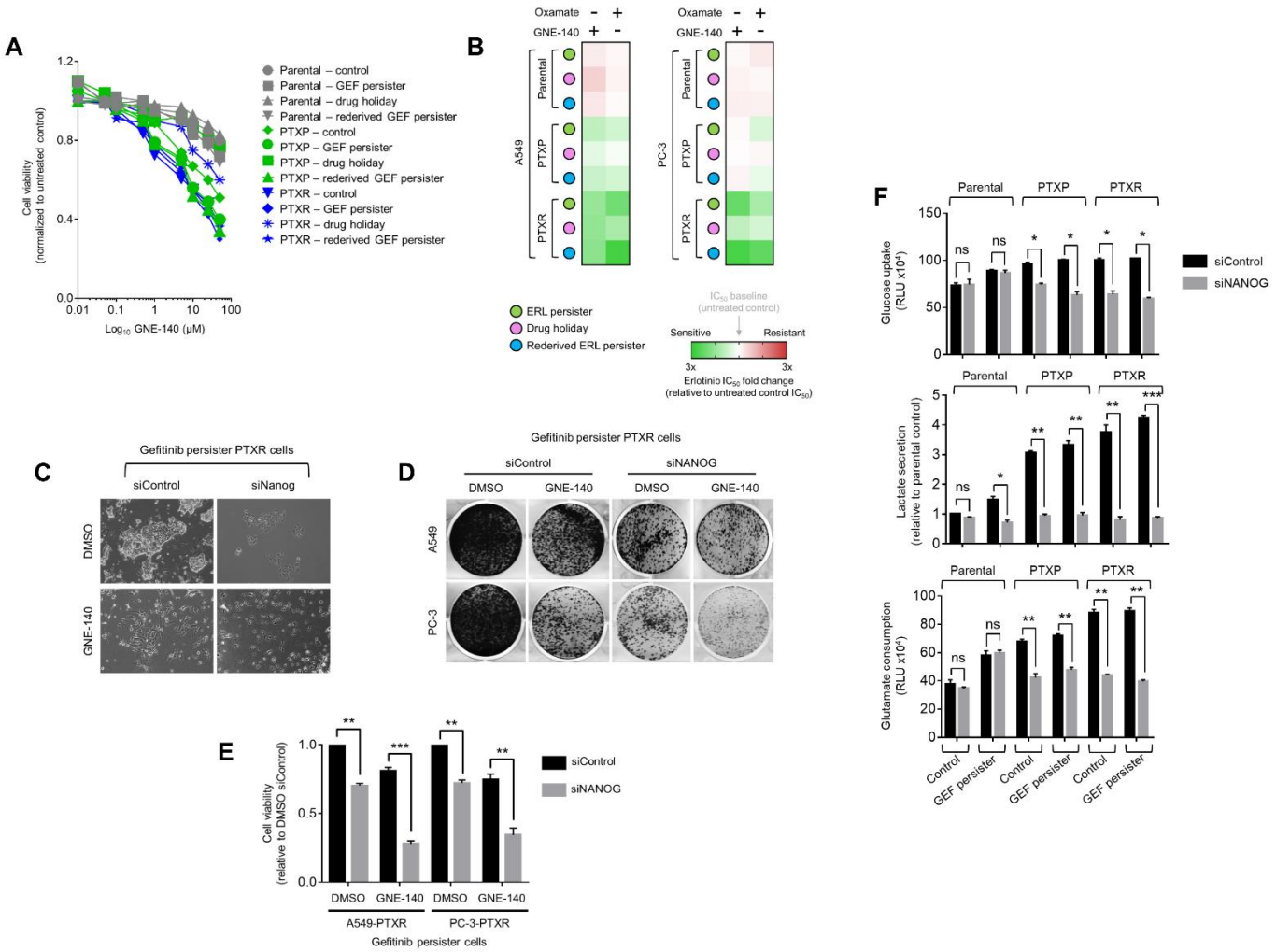

Fig. S11. Characterization of glycolysis parameters in EGFR-TKI persisters. (**A**) Sensitivity characterization upon treatment with GNE-140 in indicated A549-derived gefitinib persisters. Cells were assayed for SRB upon treatment with the indicated concentrations of GNE-140 for 72 h. Values represent measurements from four replicates and were normalized to untreated cells. (**B**) Erlotinib resistance fold in indicated A549- and PC-3-derived erlotinib persisters upon treatment with or without LDHA inhibitors (8 μM GNE-140 or 40 mM oxamate) for 24 h. Cells were assayed for SRB and IC_{50} fold change in erlotinib was identified. (**C**) Representative phase-contrast images of A549-derived gefitinib persisters upon Nanog RNAi for 48 h followed by treatment with or without 8 μM GNE-140 for 24 h. (**D**) Colony formation assay of indicated A549- and PC-3-derived gefitinib persisters upon Nanog RNAi for 48 h and treatment with or without 8 μM GNE-140 for 24 h followed by drug-free culture for 8 days. Representative of two independent experiments. (**E**) Sensitivity characterization upon Nanog RNAi for 48 h followed by treatment with or without 8 μM GNE-140 for 24 h in A549-PTXR- and PC-3-PTXR-derived gefitinib persisters. Cells were assayed for SRB (mean±SD of three biological replicates, **P*<0.05, ***P*<0.01, ****P*<0.005, Student's *t* test). (**F**) Glucose uptake, lactate secretion, and glutamate consumption measurements in indicated PC-3-derived gefitinib persisters upon Nanog RNAi for 48 h (RLU, relative luciferase units; mean±SD of three biological replicates, **P*<0.05, ***P*<0.01, ****P*<0.005, Student's *t* test).

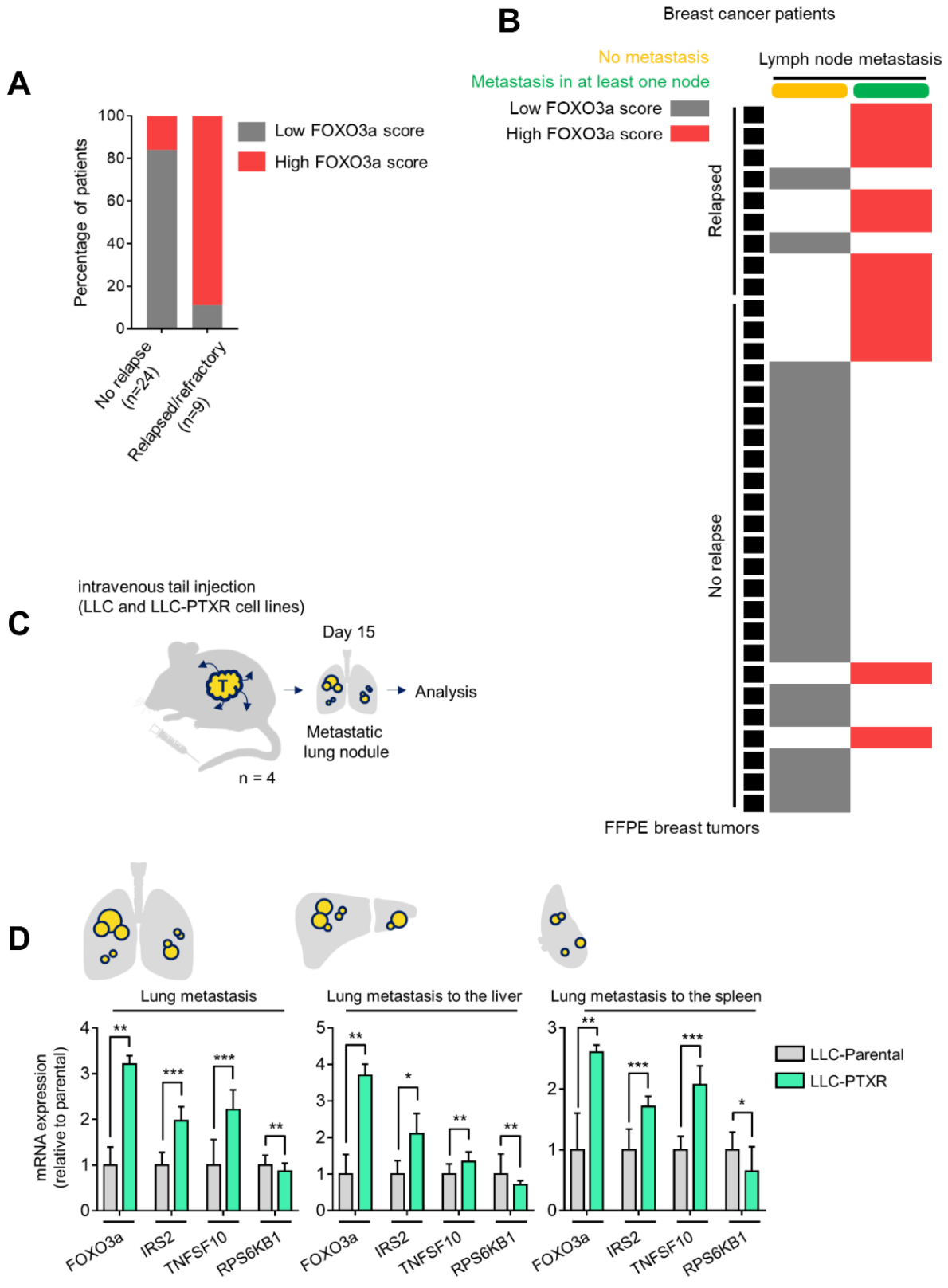

Fig. S12. FOXO3a activation is associated with the metastatic propensity of paclitaxel-resistant tumors. (**A**) Scored IHC expression of FOXO3a in FFPE tumor sections of relapsed/recurred or non-relapsed breast cancer patients. (**B**) Association of IHC FOXO3a positivity with lymph node metastasis of patients as in A (total of 33 unique patient cases). (**C**) Schematic of murine LLC metastasis model used in D. (**D**) qPCR analysis of expression of FOXO3a, its indicated target genes, and the Akt downstream target RPS6KB1 in metastatic tumor nodules from the lung, liver, and spleen of the murine metastasis model established from LLC or LLC-PTXR cells. Values are relative to parental and were normalized to GAPDH levels (mean±SD of four biological replicates, **P*<0.05, ***P*<0.01, ****P*<0.005, Student's *t* test).

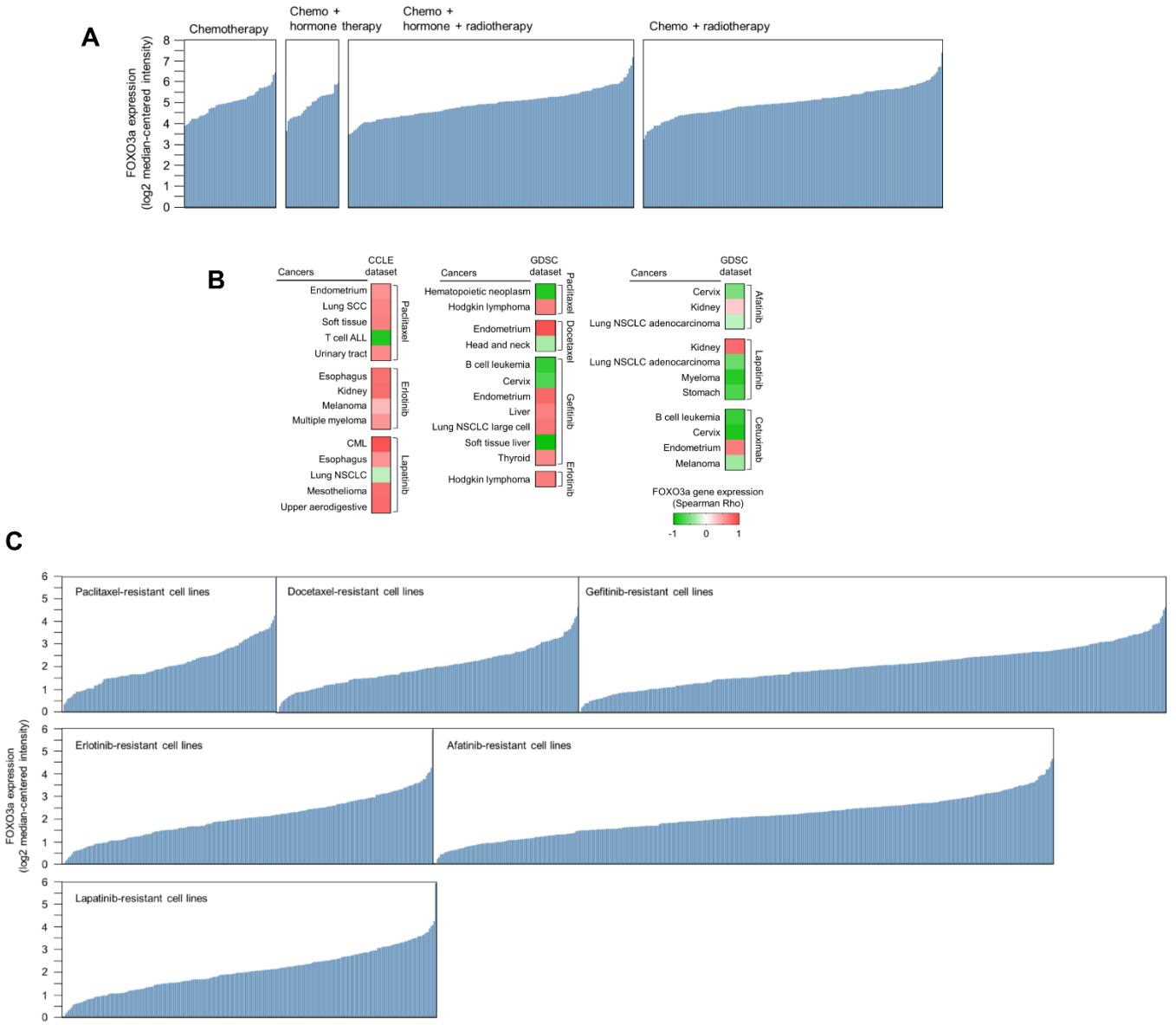

Fig. S13. FOXO3a expression is correlated with therapy relapse breast cancer patients and with drug resistance to various chemotherapy and targeted therapy agents in cancer cell lines. (**A**) Log2 transformed mRNA expression values of FOXO3 in human breast cancer patient tumors categorized per indicated treatment cohort were queried from the Oncomine database (http://www.oncomine.org) using the publicly available data set from Curtis et al., 2012 (Nature) with reporter ID ILMN_1681703. (**B**) *In silico* prediction of drug efficacy correlated with FOXO3a expression. (**C**) Log2 transformed mRNA expression values of FOXO3 in drug-resistant human cancer cell lines categorized per indicated drug resistance were queried from the same database as in A using publicly available data set from Garnett et al., 2012 (Nature) with reporter ID 204132_s_at.

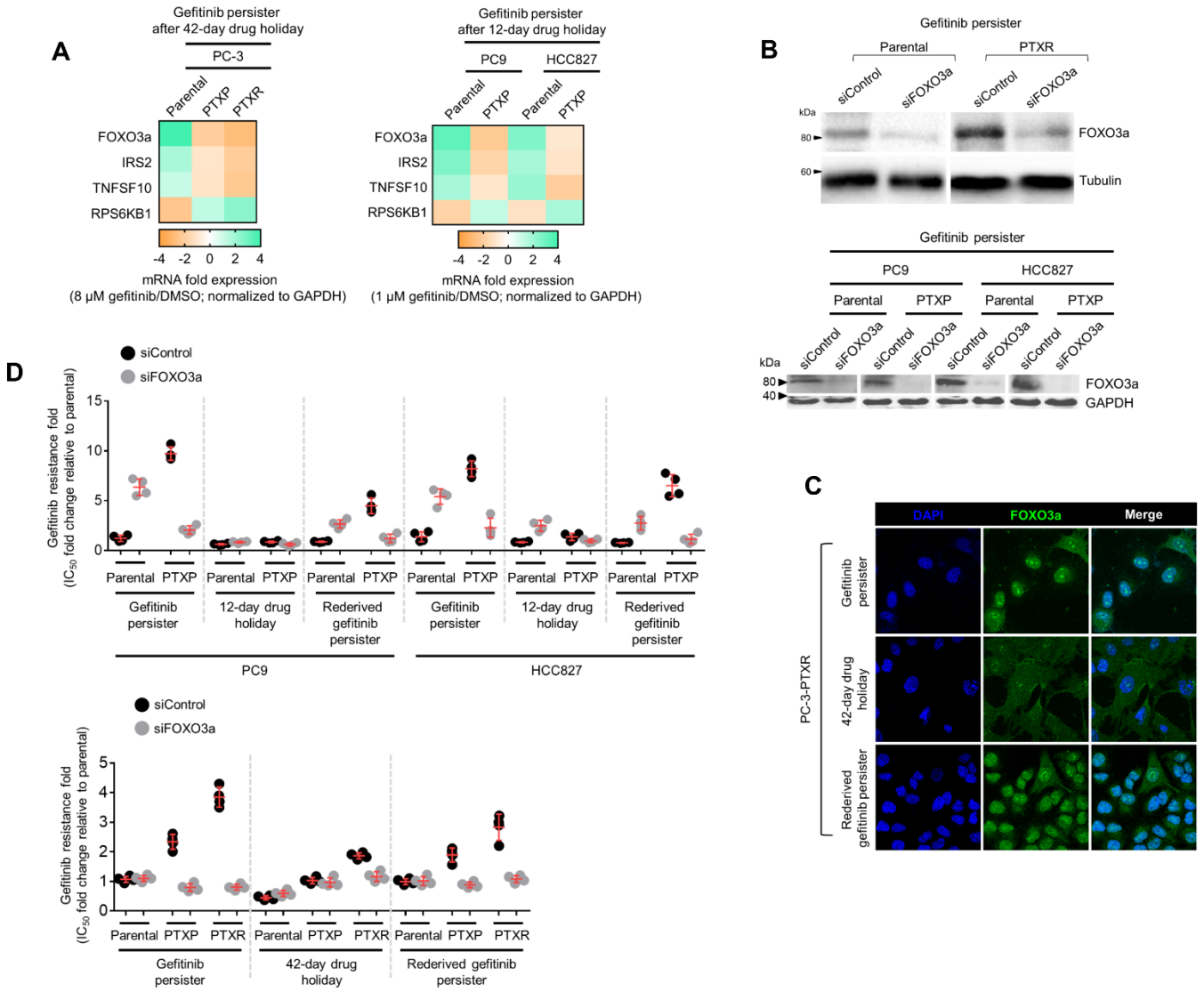

Fig. S14. Consequences of FOXO3a inhibition in GPs derived from transient and stable paclitaxel-resistant cells. (**A**) qPCR analysis of expression of FOXO3a, its indicated target genes, and the Akt downstream target RPS6KB1 in indicated sensitized PC-3-, PC9-, and HCC827-derived gefitinib persisters (after 42-day or 12-day drug holiday) upon treatment with 8 μM or 1 μM gefitinib for 72 h. Values are relative to DMSO and were normalized to GAPDH levels. Representative of two independent experiments. (**B**) Western blot analysis of FOXO3a expression in indicated PC-3-, PC9-, and HCC827-derived gefitinib persisters upon FOXO3a RNAi for 48 h. Tubulin or GAPDH was used as a loading control. Representative of two independent experiments. (**C**) Characterization of FOXO3a translocation (green) in indicated PC-3-derived gefitinib persisters by immunofluorescence upon FOXO3a RNAi for 48 h. Cells were counterstained for DAPI (blue). Representative of two independent experiments. (**D**) Gefitinib resistance characterization of indicated PC-3-, PC9-, and HCC827-derived gefitinib persisters upon FOXO3a RNAi for 48 h following gefitinib treatment for 72 h with a concentration dilution series and were assayed for SRB. Values are relative to parental control (mean±SD of four biological replicates).

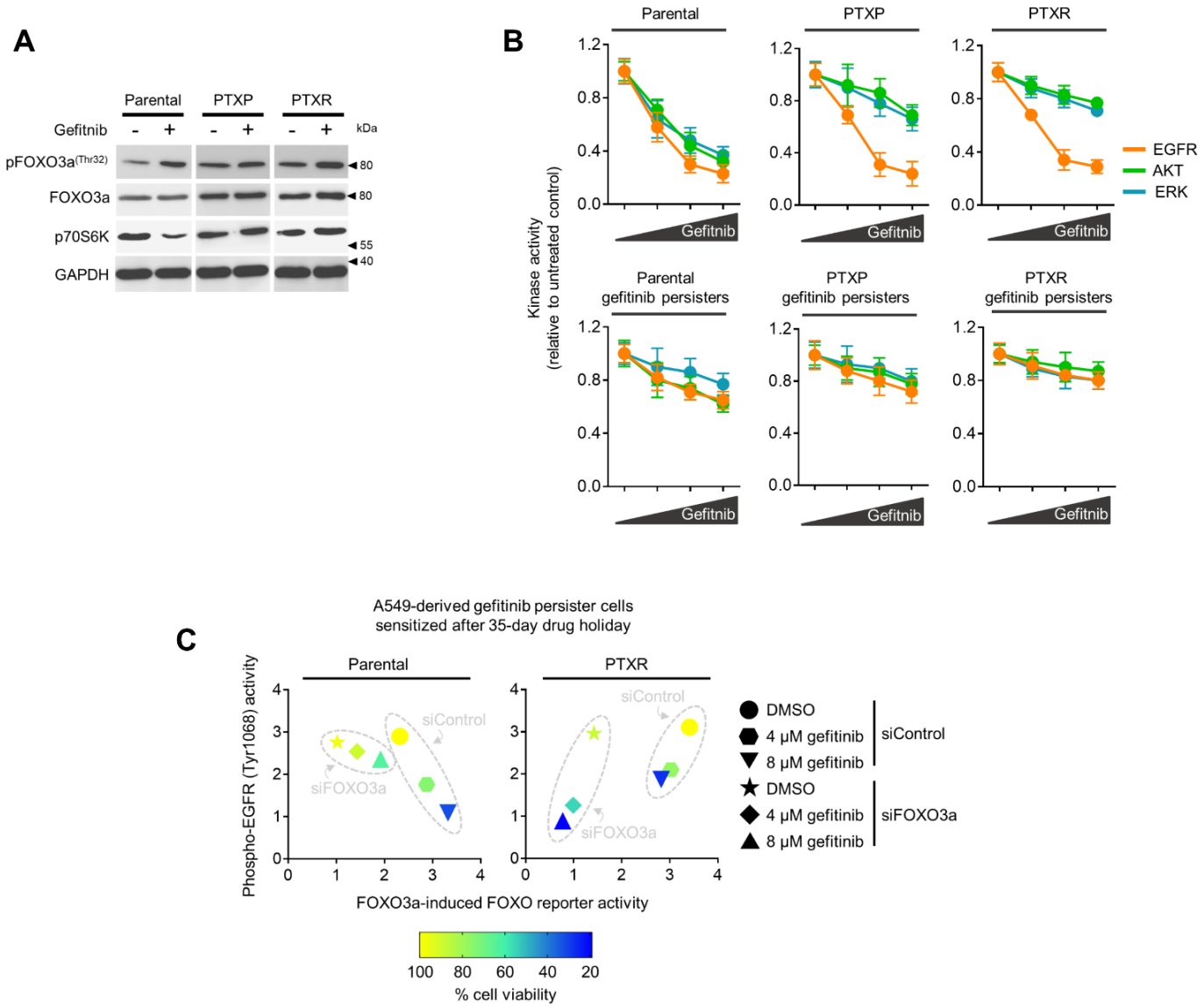

Fig. S15. FOXO3a affects protein kinase activities of EGFR and downstream signaling to facilitate apoptosis rewiring in PTXR-derived GPs. (**A**) Western blot analysis of FOXO3a threonine 32 phosphorylation, FOXO3a, and p70S6K expressions in A549-derived parental, PTXP, and PTXR cells upon treatment with or without 8 μM gefitinib for 72 h. GAPDH was used as a loading control. Representative of two independent experiments. (**B**) Luminescence-based kinase assay for EGFR, AKT, and ERK in A549-derived parental, PTXP, PTXR, and indicated gefitinib persisters upon treatment with or without increasing concentrations (4 μM, 8 μM, and 16 μM) of gefitinib for 21 h (mean±SD of two biological replicates). (**C**) ELISA sandwich-based measurement of EGFR tyrosine 1068 phosphorylation, FOXO reporter activity induced by FOXO3, and cell viability of sensitized A549- and A549-PTXR-derived gefitinib persisters upon FOXO3a RNAi for 48 h followed by treatment with or without indicated concentrations of gefitinib for additional 36 h. Representative of three independent experiments.

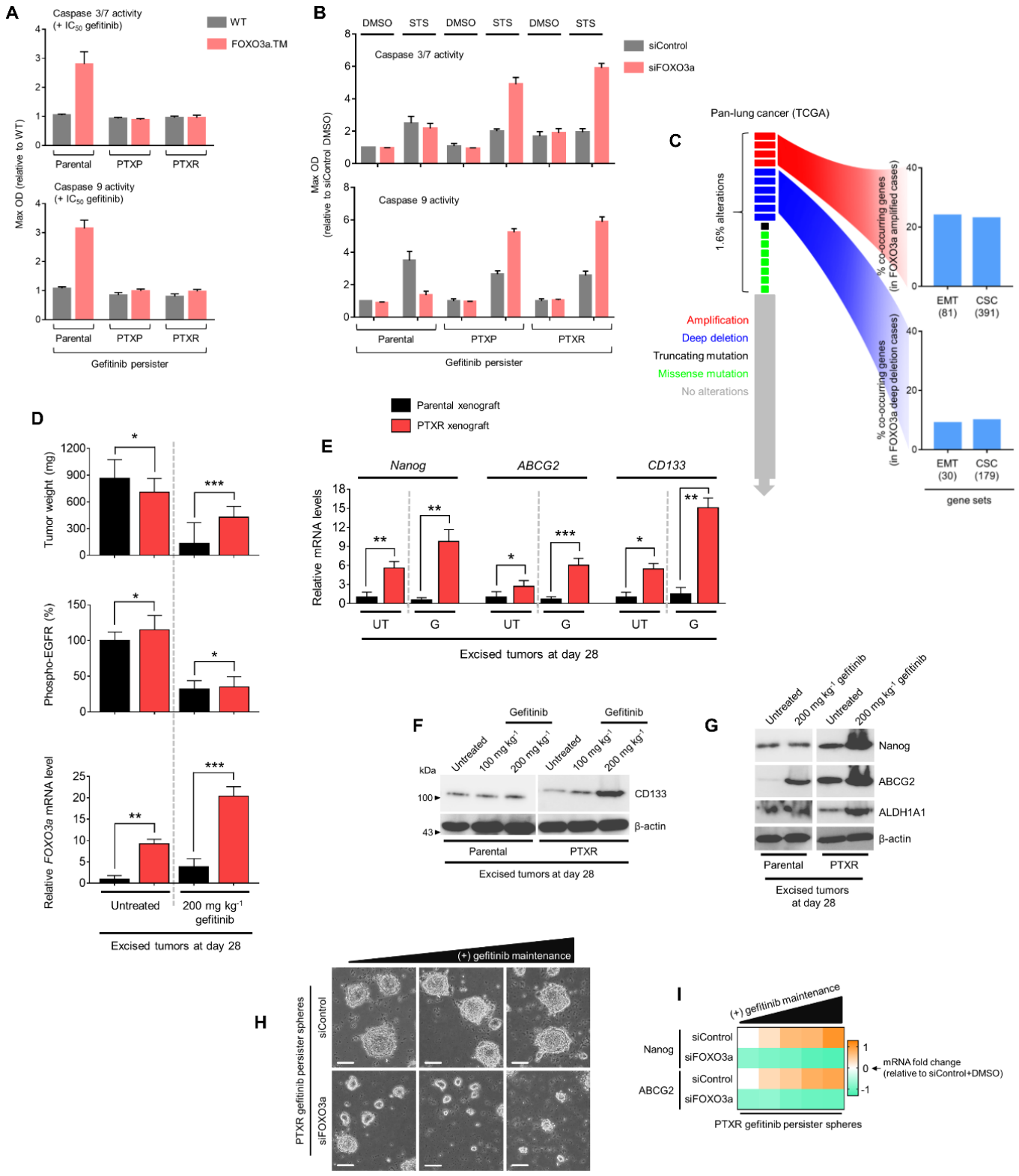

Fig. S16. Phenotypic consequences of FOXO3a inhibition on the state of apoptosis and stemness. (**A**) Caspase 3/7 DEVDase and caspase 9 activities of indicated A549-derived gefitinib persisters upon transfection with control or HA-tagged FOXO3a.TM plasmid for 36 h following treatment with varying IC_{50} concentrations of gefitinib in indicated cell lines for 72 h. Values are relative to parental control (mean±SD of three biological replicates). (**B**) Caspase 3/7 DEVDase and caspase 9 activities of indicated A549-derived gefitinib persisters upon FOXO3a RNAi for 48 h following treatment with or without 100 nM STS for 18 h. Values are relative to parental control (mean±SD of three biological replicates). (**C**) OncoPrint visualizing FOXO3a alterations across the pan-lung cancer TCGA database along with co-occurrence analysis of FOXO3a amplification and deep deletion with EMT- (out of 342 genes) and CSC- (out of 1782 genes) associated genes, respectively. (**D**, upper panel) Tumor weights upon tumor excision at day 28 of the xenografts detailed in fig. S3B (mean±SD, n=4 per cohort, **P*<0.05, ***P*<0.01, ****P*<0.005, Student's *t* test). (D, middle panel) ELISA sandwich-based measurement of EGFR tyrosine 1068 phosphorylation in the same tumor samples as in the upper panel. Values are relative to parental untreated (mean±SD of four

biological replicates). (D, lower panel, and **E**) qRT-PCR analysis of expression of FOXO3a and indicated stemness markers in the same tumor samples as in D. Values are relative to parental untreated and were normalized to GAPDH levels (mean±SD of four biological replicates, **P*<0.05, ***P*<0.01, ****P*<0.005, Student's *t* test). UT, untreated; G, 200 mg/kg gefitinib. (**F** and **G**) Western blot analysis of expression of indicated stemness markers CD133, Nanog, ABCG2, and ALDH1A1 in the same tumor samples as in D, except in panel F where 100 mg/kg gefitinib treated sample was included. β-actin was used as a loading control. Representative of two independent experiments. (**H**) Sphere formation of A549-PTXR-derived gefitinib persisters (generated in our 3D culture) during 3-day drug maintenance in gefitinib (4 μM, 8 μM, and 16 μM, respectively) upon FOXO3a RNAi for 48 h. 3D-cultured cell spheres were re-plated after RNAi followed by drug maintenance. Scale bar, 60 μm. Representative of two independent experiments. (**I**) qPCR analysis of expression of indicated stemness markers in 3D spheres derived as in H. Conditions were the same as in H, except gefitinib concentrations used were 4 μM, 8 μM, 16 μM, and 32 μM, respectively. Values are relative to siControl DMSO and were normalized to GAPDH levels (mean±SD of two biological replicates). Representative of two independent experiments.

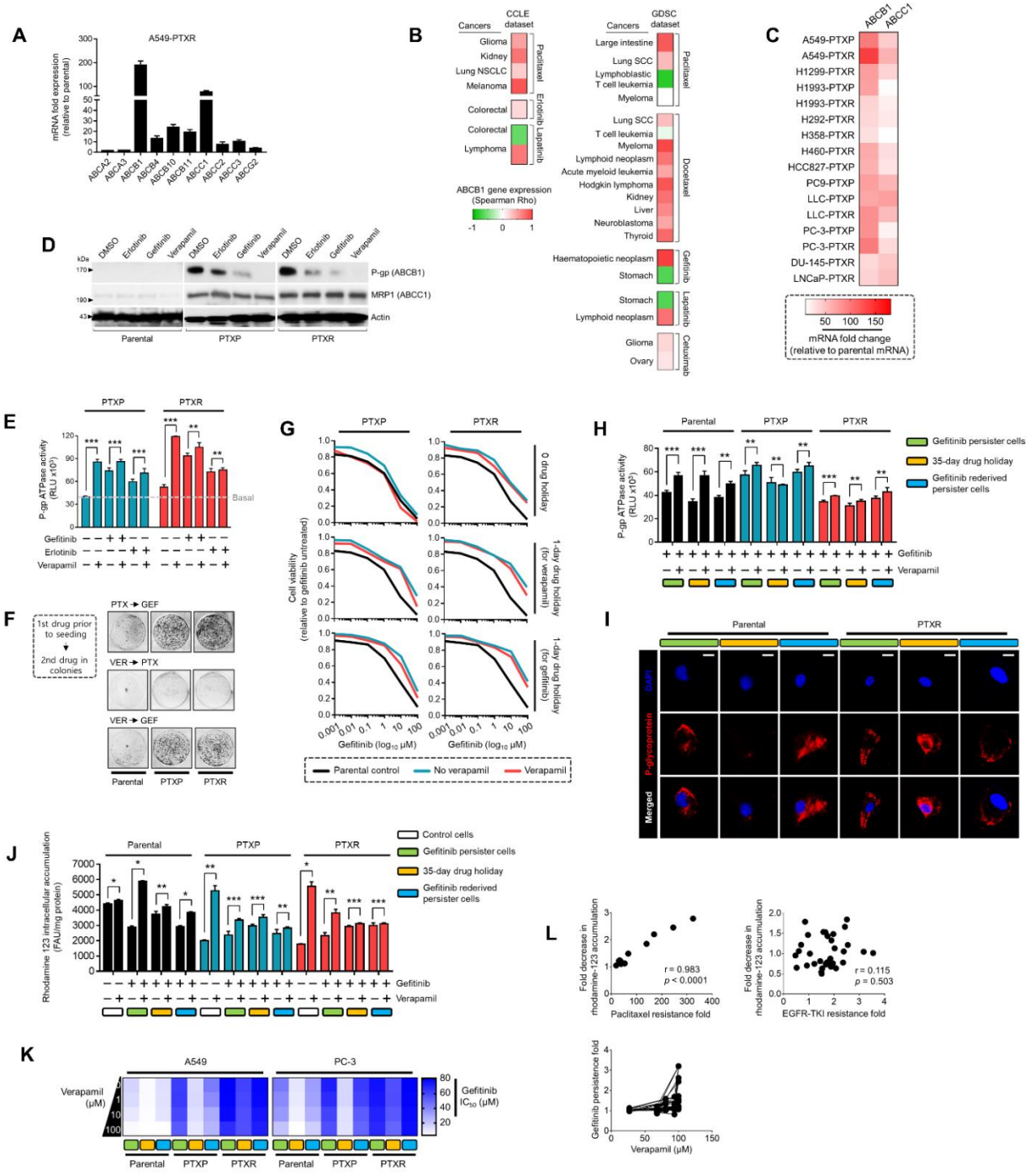

Fig. S17. Expression and activity of ABC drug efflux pumps are not required for a more stable secondary EGFR-TKI resistance. (**A**) qRT-PCR-based screening of ABC cassette genes associated with stable paclitaxel resistance in A549-PXR cells. Values are relative to parental and were normalized to GAPDH levels (mean±SD of four biological replicates). (**B**) *In silico* prediction of drug efficacy correlated

with ABCB1 expression in GDSC and Cancer Cell Line Encyclopedia (CCLE) data sets. Red and green represent positive and negative Spearman's rank correlation coefficients, respectively, between ABCB1 expression and IC_{50} of indicated drugs. (**C**) Heatmap representing ABCB1 and ABCC1 gene expressions (highest expressing transcripts from ABC gene screening as shown in A) generated from qRT-PCR in the indicated panel of PTXP and PTXR cells. Values are relative to parental and were normalized to GAPDH levels. Representative of two independent experiments. (**D**) Western blot analysis of P-gp and MRP1 in A549- derived parental, PTXP, and PTXR cells upon treatment with or without erlotinib (8 μM), gefitinib (5 μM), and verapamil (30 μM) for 24 h. Representative of two independent experiments. Actin was used as a loading control. (**E**) P-gp ATPase activities in A549-PTXP and -PTXR cells upon treatment with or without gefitinib (5 μM), erlotinib (8 μM), and verapamil (30 μM) for 4 h (RLU, relative luciferase units; mean±SD of three biological replicates, **P*<0.05, ***P*<0.01, ****P*<0.005, Student's *t* test). (**F**) Colony formation assay of A549-parental, -PTXP, and -PTXR cells following indicated drug treatment regimes (DMSO, 10 nM paclitaxel, 5 μM gefitinib, or 30 μM verapamil for 72 h as first treatment followed by re-seeding and treated with or without 4 nM paclitaxel, 2 μM gefitinib, or 10 μM verapamil for 8 days followed by drug-free culture for 4 days). Representative of two independent experiments. (**G**) Sensitivity characterization of A549-PTXP and -PTXR cells upon treatment with or without the indicated concentrations of gefitinib and 30 μM verapamil for 72 h (assayed by SRB). Values for A549-parental cells treated with or without gefitinib are also plotted for comparison. Values are relative to untreated (mean±SD of two biological replicates). (**H**) P-gp ATPase activities in indicated A549-derived gefitinib persisters treated and assayed as in e (RLU, relative luciferase units; mean±SD of two biological replicates, **P*<0.05, ***P*<0.01, ****P*<0.005, Student's *t* test). (**I**) Representative images of P-gp immunofluorescence (red) in indicated A549-derived gefitinib persisters. Nuclei are shown in blue (DAPI). Scale bar, 15 μm. Representative of two independent experiments. (**J**) Rhodamine-123 (rho-123) uptake assay in the same cells and treatments as in H. Intracellular accumulation of rho-123 is expressed as fluorescence arbitrary unit (FAU)/mg protein (mean±SD of two biological replicates, **P*<0.05, ***P*<0.01, ****P*<0.005, Student's *t* test). (**K**) Gefitinib resistance characterization upon treatment with or without the indicated concentrations of drugs for 24 h or 72 h in A549- and PC-3-derived gefitinib persisters (verapamil as first treatment for 24 h followed by gefitinib for 72 h with a concentration dilution series; assayed by SRB). Representative of two independent experiments. (**L**) Correlation between: paclitaxel resistance and decrease in rho-123 accumulation (top left panel, data separately generated in our panel of PTXP and PTXR cell lines); EGFR-TKI resistance and decrease in rho-123 accumulation (top right panel, data from J); gefitinib persistence and concentration-dependent P-gp inhibition by verapamil (bottom panel, data from K).

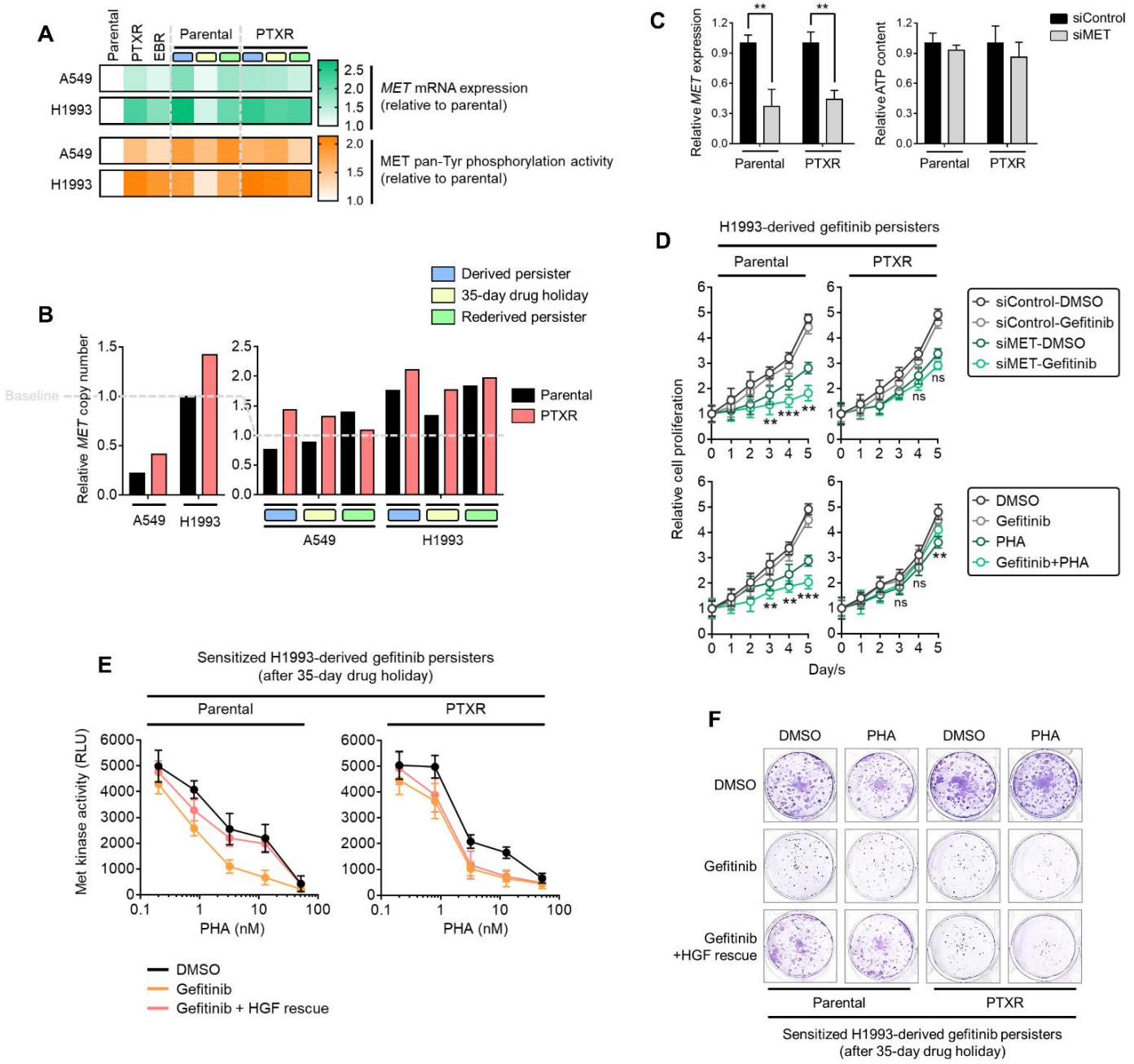

Fig. S18. MET amplification is dispensable for entering gefitinib persistence in paclitaxel-resistant cancer cells. (**A**) qRT-PCR analysis of MET expression (top panel) and ELISA sandwich-based measurement of pan tyrosine phosphorylation of Met (bottom panel) in indicated A549- and H1993-derived cells. Representative of two independent experiments. (**B**) qPCR-based assay for *MET* copy number evaluation in the same panel of cells as in A. Representative of two independent experiments. (**C**) Characterization of MET expression and ATP levels upon MET RNAi for 48 h in H1993-derived gefitinib persisters. Values represent mean±SD of three biological replicates, **P*<0.05, ***P*<0.01, ****P*<0.005, Student's *t* test. (**D**) Relative cell proliferation of indicated H1993-derived gefitinib persisters upon MET RNAi for 48 h followed by treatment with or without 8 μM gefitinib for indicated time points (top panel); or upon treatment with or without 1 μM PHA665752 for 48 h followed by treatment with or without 8 μM gefitinib for indicated time points (bottom panel). Values represent mean±SD of three biological replicates, **P*<0.05, ***P*<0.01, ****P*<0.005, Student's *t* test. (**E**) Met kinase enzyme activity of indicated sensitized H1993-derived gefitinib persisters treated with or without 8 μM gefitinib only or pretreated with 8 μM gefitinib for 24 h then followed by treatment with 40 ng/mL human recombinant HGF for 12 h. All cells were then treated with various concentrations of PHA665752 for 24 h (mean±SD of three biological replicates). (**F**) Colony formation of same cells and conditions as in D except cells were subsequently treated with 1 μM PHA665752 for 48 h followed by drug-free culture for 12 days. Representative of two independent experiments.

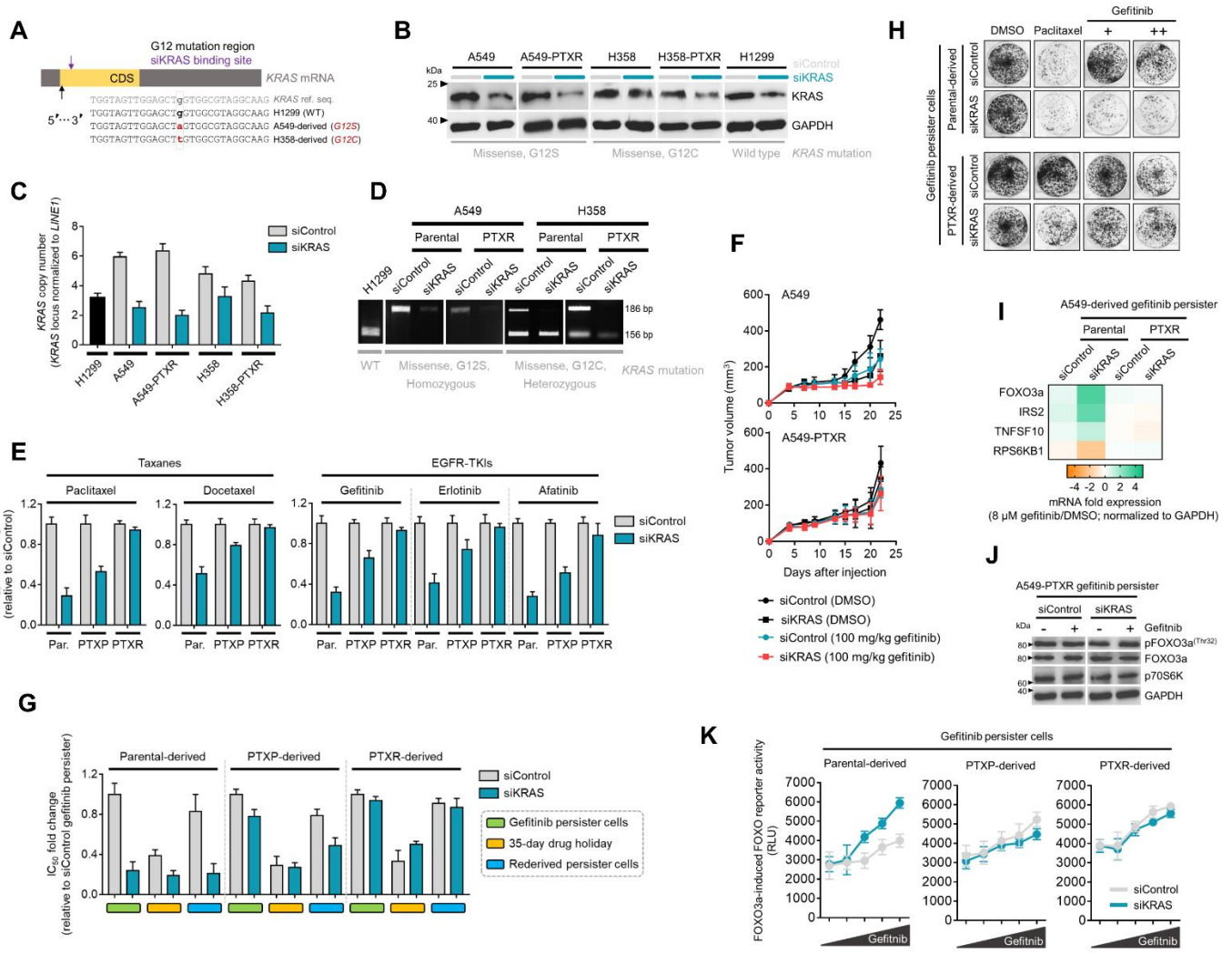

Fig. S19. Mutant KRAS is dispensable for collateral EGFR-TKI persistence development in paclitaxel-resistant cancer cells. (**A**) Binding sites of KRAS siRNA sequence (violet) used in this study in close proximity to the region of G12 and G13 codon mutations demonstrated in the coding sequence (CDS) of a mature KRAS mRNA map. (**B**) Western blot analysis of KRAS expression in indicated *KRAS* mutant A549-, H358-, and wild type (WT) H1299-derived cells upon KRAS RNAi for 60 h. (**C**) *KRAS* copy number analysis in the same panel of cells as in B upon KRAS RNAi for 60 h. (**D**) Visualization of *KRAS* WT and mutant transcripts of the same panel of cells as in B following KRAS amplification with primers designed to introduce base substitution creating a BstNI recognition site specific for the WT codon 12 but not for the codon with KRAS mutation. BstNI digestion cuts the WT allele (in H1299 cells) to produce a 156 bp fragment whereas the mutant allele remains uncut to produce a 186 bp fragment (in A549- and H358-derived cells). Note that only the mutant bands were observed in A549-derived cells as they harbor homozygous G12 codon mutation. (**E**) Taxane and EGFR-TKI resistance characterization of indicated A549-derived cells upon KRAS RNAi for 60 h following gefitinib treatment for 72 h with a concentration dilution series and were assayed for SRB. Values are relative to siControl (mean±SD of three biological replicates). (**F**) Tumor growth of A549-derived parental and PTXR cells upon subcutaneous injection into left and right flanks of nude mice. 100 mg/kg gefitinib was administered orally once daily for 14 days (top panel). The control group was treated with an equal volume of vehicle. Tumor volume was measured using digital calipers every 2~3 days and indicated time points were selected for plotting (n=3 per group, two cohorts per cell line, mean±SD, **P*<0.05, ***P*<0.01, ****P*<0.001, Student's *t* test). (**G**) Gefitinib resistance characterization of indicated A549-derived gefitinib persisters following the same KRAS RNAi and treatment schemes as in E. Values are relative to siControl (mean±SD of three biological replicates) (**H**) Colony growth of A549-derived gefitinib persisters upon the same KRAS RNAi as in E and maintenance with or without 5 μM (+) or 8 μM (++) gefitinib for 5 days or 0.5 nM paclitaxel for 4 days followed by 2 weeks of drug-free culture. Representative of two independent experiments. (**I**) qPCR analysis of expression of FOXO3a and its indicated target genes in A549-derived gefitinib persisters upon the same KRAS RNAi as in E followed by treatment with 8 μM gefitinib for 72 h. Values are relative to siControl DMSO and were normalized to GAPDH levels. Representative of two independent experiments. (**J**) Western blot analysis of FOXO3a threonine 32 phosphorylation, FOXO3a, and p70S6K expressions in A549-PTXR-derived gefitinib

persisters upon the same KRAS RNAi as in E followed by treatment with or without 8 μM gefitinib for 72 h. GAPDH was used as a loading control. Representative of two independent experiments. (**K**) FOXO reporter activity induced by FOXO3 in indicated A549-derived gefitinib persisters upon the same KRAS RNAi as in E followed by treatment with or without 4 μM, 8 μM, 16 μM, and 32 μM gefitinib for 72 h (RLU, relative luciferase units; mean±SD of three biological replicates).

A

	IC_{50} μM					
	A549	A549-PTXR	PC-3	PC-3-PTXR	LLC	LLC-PTXR
5-fluorouracil	9.8	28.9	13.8	35.8	4.7	22.3
Cisplatin	18.9	37.7	9	26.7	0.3	0.6
Carboplatin	22.4	36.1	37.6	56.5	12	32.2
Gefitinib	5.7	35.3	15.5	47.8	2.1	16.3
Erlotinib	11.9	33.9	9.3	29.2	1.4	9.7
Afatinib	5	21	12	32.7	0.8	2
Lapatinib	0.9	2.9	4.5	9	2.9	3.9
PHA665752	6.4	14.1	8.5	13.9	18	31
Cabozantinib	4.8	8.9	10.6	21.1	6.7	17
BMS777607	5.3	9.5	27.6	32.7	6	6.5
Crizotinib	5.4	10.2	3.7	9.9	1.4	5.2
Vemurafenib	7.3	0.2	1.7	1.5	9	0.1
PD173074	4	1.6	7.6	0.5	7	0.9
Sunitinib	1	0.06	4	0.07	1.8	0.09

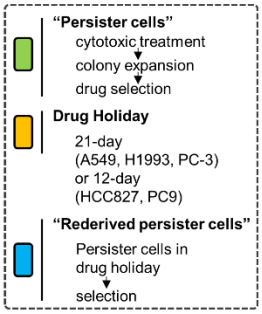

B

		selected from maximum tolerated concentration			selected from minimal tolerated concentration			
		Parental	PTXP	PTXR	Parental	PTXP	PTXR	
A549-derived	Gefitinib persister cells	52.2	160.9	265	18.2	67.4	103.4	Gefitinib IC_{50} μM
		17.3	42.9	180.8	4.9	30.2	68.1	
		47.1	126.2	252.6	10.7	40.4	74.6	
	Erlotinib persister cells	169.8	282.6	566.4	78.4	85.1	130.5	Erlotinib IC_{50} μM
		95.1	177	322.5	35.3	26.5	97.7	
		153	247.6	520.5	50.7	51.1	111.1	
H1993-derived	Gefitinib persister cells	4.8	42.2	68.8	3.2	29.3	43.6	Gefitinib IC_{50} μM
		1.4	6.8	10.6	0.8	5.3	5.8	
		4.4	31.8	58.2	2.5	20.1	31.2	
	Erlotinib persister cells	26.9	81.1	90.4	9.4	31.9	40.7	Erlotinib IC_{50} μM
		2.9	12.9	14.7	0.7	8.2	7.3	
		17.5	57.8	72	3.5	20.4	25.1	
PC-3-derived	Gefitinib persister cells	191.8	668.3	740.4	47.2	223.1	266.2	Gefitinib IC_{50} μM
		57.6	168.9	193.3	17	32.9	83.4	
		168.3	618.8	716.1	44.28	112.3	209.9	
	Erlotinib persister cells	196.3	337	348.1	57.4	97.7	198.2	Erlotinib IC_{50} μM
		67.8	72.4	68.9	15.3	29.2	40.9	
		154.9	273.4	310	38.8	91.8	144.1	

C

	A549-derived			H1993-derived			PC-3-derived			
	selected from maximum tolerated concentration									
	Parental	PTXP	PTXR	Parental	PTXP	PTXR	Parental	PTXP	PTXR	
Gefitinib persister cells	5.7	11.4	36.2	2.9	19.4	21.6	11.9	38.2	90.1	Afatinib IC_{50} μM
	4.4	9.4	26.8	1.9	8.5	11.3	10.5	34.8	83.8	
	4.7	10.1	27.1	2.1	9.2	14.5	11.5	34.4	83.5	
	1.7	2.8	8.2	0.1	0.2	0.7	7.8	15.1	21.4	Lapatinib IC_{50} μM
	0.7	2.1	5.7	0.08	0.1	0.3	6.8	10.4	15.3	
	1.1	2.6	6.4	0.1	0.2	0.6	7.6	14	19.1	
	Parental	PTXP	PTXR	Parental	PTXP	PTXR	Parental	PTXP	PTXR	
Erlotinib persister cells	4.6	27.1	77.3	4	17.9	22.2	14.9	34.4	86.8	Afatinib IC_{50} μM
	4	23.7	72.1	2.3	9.3	13.5	12.8	29.5	85.5	
	4.2	25.3	73.6	2.4	11.3	15.5	12.3	30.2	81.1	
	1.4	3.8	8.4	0.1	0.2	0.6	7.4	15.4	20.5	Lapatinib IC_{50} μM
	0.7	2.1	6.1	0.09	0.1	0.2	3.9	11.5	16.2	
	1.2	3.2	8.3	0.1	0.2	0.5	6	14.3	21.6	

D

		A549-derived			PC-3-derived			
		selected from minimum tolerated concentration						
		Parental	PTXP	PTXR	Parental	PTXP	PTXR	
GNE-140-treated	Gefitinib persister	22.9	46.4	33.4	57.6	106.7	66.9	Gefitinib IC_{50} μM
		5.6	35.5	37.4	24.7	39.8	81.7	
		14.8	22.6	28	57.7	67.6	77.7	
	Erlotinib persister	97.2	45.5	61.8	63.1	101.6	74.2	Erlotinib IC_{50} μM
		69.5	20.2	48.6	17.5	29.7	21.7	
		65.4	28.3	53.1	46.1	101.8	50.7	
		Parental	PTXP	PTXR	Parental	PTXP	PTXR	
Oxamate-treated	Gefitinib persister	23.8	80.2	29	55.6	168.7	95	Gefitinib IC_{50} μM
		5.9	32.7	56.5	20.4	36.7	92.4	
		11.7	44	25	54	93.6	172	
	Erlotinib persister	86.2	47.8	51.1	72.8	70.7	138.6	Erlotinib IC_{50} μM
		40.2	24.5	49.3	16.9	30.6	30.2	
		54.7	29.3	38.4	45	78.4	57.1	

E

	PC9-derived		HCC827-derived		
	Parental	PTXP	Parental	PTXP	
Gefitinib persister cells	0.35	18.3	0.18	2.0	**Gefitinib** IC_{50} μM
	0.08	2.8	0.04	0.69	
	0.33	12.5	0.16	1.48	
	0.14	3.49	0.03	0.52	**Erlotinib** IC_{50} μM
	0.07	1.84	0.02	0.19	
	0.08	3.1	0.02	0.37	
	0.14	3.58	0.04	0.32	**Afatinib** IC_{50} μM
	0.13	3	0.04	0.29	
	0.12	3.22	0.04	0.31	
	0.09	1.49	0.03	0.31	**Lapatinib** IC_{50} μM
	0.08	1.42	0.03	0.29	
	0.08	1.71	0.04	0.29	

Fig. S20. Calculated IC_{50} values. Calculated IC_{50} values from experiments detailed in (**A**) Fig. 1E, (**B**) Fig. 2A, (**C**) Fig. 2B, (**D**) Fig. 4H, fig. S11B, and (**E**) fig. S8B.

Table S1. Clinicopathologic information of human breast cancer patients.

Study ID	SNU Pathology ID	Subnumber	Age	Nuclear grade	Histologic grade	Tumor size	Lymph node metastasis	Recurrence/relapse
12	S 130000238	4	36	3/3	III/III	5.1 x 5.0 x 3.0cm, 2.2 x 1.4 x 1.5cm	metastasis in one out of 28 lymph nodes	O
1	S 130001251	2	41	3/3	III/III	3.8 x 3.5 x 4.5cm	metastasis in one out of 10 lymph nodes	N/A
2	S 130001476	26	44	3/3	II/III	up to 2.3 x 1.1cm	metastasis in two out of 16 lymph nodes	X
11	S 130001591	2	31	3/3	II/III	1.8 x 1.2 x 3.0cm	metastasis in one out of 22 lymph nodes	O
3	S 130004803	2	48	3/3	II/III	up to 2.1 x 1.4 x 2.0cm	metastasis in ten out of 24 lymph nodes with extracapsular extension	X
4	S 130007746	16	65	3/3	II/III	4.1 x 1.7 x 2.0cm	metastasis in three out of 19 lymph nodes	X
10	S 130021253	1	66	3/3	III/III	4.8 x 3.6 x 3.5cm	no metastasis in 19 lymph nodes	O
9	S 130027215	7	43	3/3	III/III	4.5 x 2.7 x 4.0cm	no metastasis in 5 lymph nodes	O
5	S 130044283	1	62	3/3	III/III	up to 1.9 x 1.6 x 2.5cm	metastasis in one out of nine lymph nodes	X
6	S 130066972	1	45	3/3	III/III	up to 4.8 x 3.8 x 3.0cm	no metastasis in five lymph nodes	N/A
31	S 130000525	3						O
7	S 140035725	10	47	3/3	III/III	up to 0.3 x 0.3 x 0.5cm	metastasis in five out of 15 lymph nodes	O
13	S 140042446	2	57	3/3	III/III	0.3 x 0.2cm	no metastasis in five lymph nodes	X
33	S 140044709	11	26	3/3	III/III	up to 0.2 x 0.2 x 0.2cm	no metastasis in nine lymph nodes	O
14	S 140052380	6	42	2/3	II/III	0.2 x 0.2 x 0.2cm and 0.1 x 0.1 x 0.1cm	no metastasis in seven lymph nodes	X
15	S 140052695	3	58	2/3	III/III	0.3 x 0.2 x 0.2cm	no metastasis in nine lymph nodes	X
16	S 140058841	11	40	2/3	II/III	up to 0.4 x 0.3cm	metastasis in one out of 14 lymph nodes	X
32	S 140060207	15	63	2/3	II/III	up to 0.3 x 0.2cm	no metastasis in 11 lymph nodes	O
17	S 140066763	10	56	3/3	III/III	0.4 x 0.3 x x0.5 cm	0/3	X
18	S 150000211	2	51	2/3	II/III	up to 0.4 x 0.4 cm	3 with extracapsular extension/13	X
19	S 150016655	14	53	3/3	III/III	0.4 x 0.4 x 0.4cm	no metastasis in eight lymph nodes	X
20	S 150030142	11	48	3/3	II/III	up to 0.2 x 0.2 x 0.2 cm	4/14	X
21	S 150045141	8	37	2/3	II/III	0.3 x 0.3cm	0/3	X
22	S 150052114	10	42	2/3	II/III	0.3 x 0.2cm	no metastasis in 21 lymph nodes	X
23	S 150053706	8	38	2/3	II/III	up to 0.3 x 0.2cm	metastasis in 11 out of 20 lymph nodes	X
24	S 150068908	1	31	3/3	III/III	up to 0.2 x 0.2 cm	0/5	X
25	S 150071617	3	38	2/3	II/III	0.2 x 0.2 cm	0/4	X
26	S 160001213	33	59	2/3	II/III	up to 0.4 x 0.3cm	no metastasis in six lymph nodes	X
8	S 160002990	6	48	3/3	III/III	0.2 x 0.2 cm	0/5	O
27	S 160005609	11	31	3/3	II/III	up to 0.4 x 0.2 cm	5/12	X
28	S 160026090	2	38	3/3	III/III	0.4 x 0.3cm	no metastasis in three lymph nodes	X
29	S 160043792	10	54	2/3	II/III	0.4 x 0.3 cm	0/8	X
30	S 160049290	6	47	3/3	III/III	0.4 x 0.4 x 0.4cm	no metastasis in nine lymph nodes	X

Table S2. Primer sequences for qRT-PCR.

Target gene	Forward (5'→3')	Reverse (5'→3')
18S	CGCCGCTAGAGGTGAAATTC	TTGGCAAATGCTTTCGCTC
ABCA2	AAGCCTGTGGAGGATGATGTG	GGTCAACGGCCAGGATACG
ABCA3	CAAAACCCTGGATCACGTGTT	CCTCCGCGTCTCGTAGTTCT
ABCB1	CATCATTGCAATAGCAGG	GTTCAAACTTCTGCTCCTGA
ABCB4	TTTTTACTTTCTTCCTTCAGGGTTTC	TAAAAGCCATTGACCGCAGTCT
ABCB10	GCTTCCGTAGGCATCAGTATGAT	GGAGGCACCACGCTCAAA
ABCB11	AGGGAGCTACCAGGATAGTTTAAGG	TCGTGCACCAGGTAAGAAAGC
ABCC1	GAAGGCCATCGGACTCTTCA	CAGCGCGGACACATGGT
ABCC2	TGCAGCCTCCATAACCATGAG	GATGCCTGCCATTGGACCTA
ABCC3	CACACGGATCTGACAGACAATGA	ACAGGGCACTCAGCTGTCTCA
ABCG2 (cells)	CAGGTCTGTTGGTCAATCTCACA	TCCATATCGTGGAATGCTGAAG
ABCG2 (tumor tissues)	TCATCAGCCTCGATATTCCATCT	GGCCCGTGGAACATAAGTCTT
ACTIN	ATCAAGATCATCGCACCCCC	ACTCCTGCTTGCTGATCCAC
BMI1	CCAGGGCTTTTCAAAAATGA	CCGATCCAATCTGTTCTGGT
BMP2	ATGGATTCGTGGTGGAAGTG	GTGGAGTTCAGATGATCAGC
BMP4	AGCATGTCAGGATTAGCCGA	TGGAGATGGCACTCAGTTCA
BMP5	CCGGGATCTGGGATGGCAGGA	TGGCAGCCACATGAGCGTACT
BMP6	CAGCCTGCAGGAAGCATGAG	CAAAGTAAAGAACCGAGATG
BMP7	TGGAACATGACAAGGAATTCT	CATCCAGCGTCTCCACCGAGA
BMP9	CCTGGGCACAACAAGGAC	CCTTCCCTGGCAGTTGAG
BMP10	CTGCCAACATCATTAGGAGT	ACTGAACCTGACCGTACA
CD133	TGGATGCAGAACTTGACAACGT	ATACCTGCTACGACAGTCGTGGT
CDH1 (E-cadherin)	GAACAGCACGTACACAGCCCT	GCAGAACTGTCCCTGTCCCAG
CDH2 (N-cadherin)	GACGGTTCGCCATCCAGAC	TCGATTGGTTTGACCACGG
CHRDL2	GCCTGCTATGCTCAGTCAGTG	TCTGAAGTGGCGAGGGATGAA
CTNNB1 (β-catenin)	GTGCAATTCCTGAGCTGACA	CTTAAAGATGGCCAGCAAGC
CXCL1	AGGGAATTCACCCCAAGAAC	TGGATTTGTCACTGTTCAGCA
CXCL10	GCTGCCGTCATTTTCTGC	TCTCACTGGCCCGTCATC
FN1 (Fibronectin)	GGAAAGTGTCCCTATCTCTGATACC	AATGTTGGTGAATCGCAGGT
FOXO3A (human)	TTCAAGGATAAGGGCGACAG	CAGGTCGTCCATGAGGTTTT
FOXO3a (mouse)	TACGAGTGGATGGTGCGCTG	AGGTTGTGCCGGATGGAGTTC
GAPDH	CTCTCTGCTCCTCCTGTTCGAC	TGAGCGATGTGGCTCGGCT
GREM1	GTCACACTCAACTGCCCTGA	GGTGAGGTGGGTTTCTGGTA
IL1-α	TCCATAACCCATGATCTGGAA	TTGGTTGAGGGAATCATTCAT
IL6	GCTACCAAACTGGATATAATCAGGA	CCAGGTAGCTATGGTACTCCAGAA
IRS2 (human)	TTCTTGTCCCACCACTTGAA	CTGACATGTGACATCCTGGTG
IRS2 (mouse)	GTCCAGGCACTGGAGCTTT	GCTGGTAGCGCTTCACTCTT
KRAS	TGACCTGCTGTGTCGAGAAT	TTGTGGACGAATATGATCCAA
LIN28	TTGTCTTCTACCCTGCCCTCT	GAACAAGGGATGGAGGGTTTT
LINE1 ORF	GCTACGGGAGGACATTCAAA	TTCAGCTCCATCAGCTCCTT
LMNB1	GGGAAGTTTATTCGCTTGAAGA	ATCTCCCAGCCTCCCATT
MET	AATAGAAAACTGACAATGTTGAGAGG	TGAAATTCATCCAACCAAATCTT
MMP-3	CAAAACATATTTCTTTGTAGAGGACAA	TTCAGCTATTTGCTTGGGAAA
MMP-9	ACGACATAGACGGCATCCA	GCTGTGGTTCAGTTGTGGTG
NANOG (cells)	CCTCCTCCATGGATCTGCTTATTCA	CAGGTCTTCACCTGTTTGTAG
NANOG (tumor tissues)	AATACCTCAGCCTCCAGCAGATG	TGCGTCACACCATTGCTATTCTTC
OCT4	ACATCAAAGCTCTGCAGAAAGAACT	CTGAATACCTTCCCAAATAGAACCC
P16INK4A	AATCTCCGCGAGGAAAGC	GTCTGCAGCGGACTCCAT
RPS6KB1 (human)	GCA ATGATAGTGAGGAATGCTAAG	GCTGTGTCTTCCATGAATATTCC
RPS6KB1 (mouse)	CGTGGAGTCTGCGGCG	CATATGGTCCAACTCCCCCA
SNAI1 (Snail)	CATGTCTGGACCTGGTTCCT	AAGGGTCCTTGAGGGAGGTA
SNAI2 (Slug)	TGGTTGCTTCAAGGACACAT	GTTGCAGTGAGGGCAAGAA
SOX2	AGCTACAGCATGATGCAGGA	GGTCATGGAGTTGTACTGCA
TNFSF10 (human)	CCTCAGAGAGTAGCAGCTCACA	CAGAGCCTTTTCATTCTTGGA
TNFSF10 (mouse)	TCCAATCTCCAAGGATGGAAAGA	GATGTAATACAGGCCCTCCTGCTC
VIM (Vimentin)	TACAGGAAGCTGCTGGAAGG	ACCAGAGGGAGTGAATCCAG